# HYBRID SILICA NETWORK MODIFIED BY GOLD NANOSPHERES

By

STAMATIA KALLONTZI

A dissertation submitted to the

School of Graduate Studies

Rutgers, The State University of New Jersey

In Partial fulfillment of the requirements

For the degree of

Doctor of Philosophy

Graduate Program in Materials Science and Engineering

Written under the direction of

Lisa C. Klein

And approved by

_____

_____

_____

_____

New Brunswick, New Jersey

October, 2019

# Abstract of the Dissertation


HYBRID SILICA NETWORK MODIFIED BY GOLD NANOSPHERES

By STAMATIA KALLONTZI

Dissertation Director: Lisa C. Klein

In this study hybrid silica gels were doped by adding gold citrate nanospheres. The interface of the two components of this material and the structural differences between doped and non-doped melting gels were studied. Melting gels are a class II subgroup of Organically Modified Silicates (ORMOSILs). This type of gels has been named a melting gel (MG) after its property to soften when heated up at a certain temperature and become rigid when cooled down. This repeatable process can be performed many times until the hybrid silica network is fully crosslinked and results into a glass material.

The melting gels studied in this project were synthesized by the organoalkoxysilanes methyltriethoxysilane (MTES) and dimethyldiethoxysilane DMDES). MTES and DMDES were combined in a sol gel synthesis. Manipulating of the mono-substituted and di-substituted organoalkoxysilanes ratio is a way to control the amount of organic matter being introduced in the hybrid organic-inorganic silica network. For the preparation of the melting gel samples the molar ratios of precursors used were 65% MTES – 35% DMDES, 70% MTES – 30% DMDES, 75% MTES – 25% DMDES. During the synthesis process of MG, gold citrate nanospheres (Au-nsps) were added in the melting gel transforming colorless gel

into purple transparent gels. Gold nanospheres were added in five different concentrations as they were synthesized.

With an interest in the modifications that the nanoparticles caused to the hybrid silica network a series of analyses were performed. Vibrational spectroscopies, microscopy and small angle X-ray scattering (SAXS) was utilized to decipher how the MGs are altered by the addition of the nanoparticles. Fourier transform infrared spectroscopy (FT-IR) was used to monitor the consolidation process of both doped and non-doped melting gels. This analysis showed how the melting gel transitions from gel to glass. Raman as a complementary method to FT-IR was employed to study differences between hybrid glasses of the three different aforementioned precursor ratios. TEM was used to image the doped melting gels. Micrographs of microtomed consolidated MGs showed that the gold nanoparticles were distributed across the melting gel network. The size and shape of the monodispersed nanoparticles was not changed during the incorporation process, while some agglomerations were noticeable probably around defects of the network. SAXS performed on doped hybrid glasses confirmed the monodispersity of the Au-nsps, maintaining the size and shape, and the appearance of few agglomerations.

All the compositions exhibited different behavior indicating the formation of distinctive networks and the comparison among different compositions of Au-nsps was held with UV-Vis spectroscopy, rotational rheometry, differential scanning calorimetry (DSC) and thermogravimetric analysis (TGA). UV-Vis spectroscopy was the first analysis to confirm the maintenance of plasmonic behavior of the nanocomposite. The nanoparticles continued to absorb in UV-Visible range after their incorporation in the melting gel media. An effect to the glass transition temperature ($T_g$) was confirmed by both rotational rheometry and DSC, as the concentration of Au-nsps the $T_g$ and viscosity of 65% MTES –

35% DMDES and 75% MTES – 25% DMDES went through a minimum. Another noticeable characteristic was that non-doped melting gels in TG-DTA showed more mass loss than doped melting gels.

In conclusion, a new material was created, combining melting gels and gold citrate nanospheres. Doped melting gels inherited the main characteristics of both components, such as thermal and plasmonic properties. Gold nanospheres did affect hybrid silica network both in gel and in glass form. The study of the consolidation process gave substantial information how this transition is carried and what aspects of the hybrid silica network are changing. Lastly, incorporation of Au-nsps was depicted via TEM and confirmed by SAXS. The analysis of this unique material revealed a lot of information for glasses doped by metallic nanoparticles which will be useful in the research of doped hybrid glasses and their applications such as corrosion protection coatings.

# Acknowledgements

There has been four full years that are depicted in this dissertation. It was a period of learning, trying and not giving up. The last one is the key to reach your goals. In this journey I was lucky to have great mentors who were always available to guide me and teach me how to be a better scientist. Specifically, I would like to thank Dr. Klein for offering me this great opportunity to conduct research under her supervision and Dr. Fabris that made me a member of her group and showed me what teamwork is. Thanks to Dr. Jitianu and Dr. Tsilomelekis I was constantly challenged to broaden my research and learn new techniques. I would also like to thank all my group members for the support and the help that they offered any time I was struggling. Unequivocally, I owe to thank my family for their support and for being a great role model. Finally, I would like to thank all the people that were there with me during this journey with patience and laughs.

# Contents

## *List of Figures*

## *List of Tables*

## *List of Abbreviations*

| | |
|---|---|
| Au-nsps | Gold nanospheres |
| DMDES | Dimethyldiethoxysilane |
| DSC | Differential Scanning Calorimetry |
| DTA | Differential Thermal Analysis |
| FT-IR | Fourier Transform Infrared Spectroscopy |
| LSPR | Localised Surface Plasmon Resonance |
| MG | Melting gel |
| MTES | Methyltriethoxysilane |
| MTMS | Methyltrimethoxysilane |
| ORMOSIL | Organically Modified SIlicate |
| PhTES | Phenyltriethoxysilane |
| SAXS | Small Angle X-ray Scattering |
| SERS | Surface Enhanced Raman Spectrosxopy |
| TEOS | Tetraethoxysilane |
| TGA | Thermogravimetric Analysis |
| TMOS | Tetramethoxysilane |

# Introduction

Hybrid organic–inorganic materials were called ORMOSILs (Organically modified Silicates) for the first time in 1984 by Schmidt.[1] In the case of ORMOSILs, a silica network is modified by organic compounds during synthesis. This thesis is focused on synthesizing ORMOSILs by a sol-gel process using organically modified silicon alkoxides as precursors. Specifically the particular types of ORMOSILs under investigation are melting gels. The name of this material comes from its unique property of having a low viscosity at a certain temperature, so low that it can be poured. Hybrid gels that have this tendency to soften temporarily at a certain temperature were discovered in 1998.[2] Since then, many different melting gels have been created, primarily for use as coatings.

The objective of this project is to synthesize melting gels of varying precursor ratios, dope them with gold nanospheres and study the composite material. The main interests of this project are the modifications of either of the two components of the system after the merger. This particular type of ORMOSILs has been developed as anti-corrosion films of metal surfaces, which mandates the analysis of the thermal properties and the viscosity of the final material.

The strategy for developing new melting gels is based on the desired application of the material. In general, the sol-gel process is a useful tool which can create gels with countless different properties. Since the application of interest here is corrosion protection coatings, the ability to coat a surface is essential. The low softening temperature makes melting gels ideal coatings for glass, polymers or metals. When melting gels reach their "melting" temperature, they can be deposited via spin coating or dip coating. [3]

The second focus of this thesis is incorporating gold nanoparticles in melting gels. Metal powders have been used to give color for hundreds of years beginning in Mesopotamia. Another use for metals powders in hybrid silica gels is to control their thermal properties. Based on the hypothesis that gold nanoparticles can alter the thermal properties, gold doped melting gels were synthesized. A synthesis process was used that generated a homogeneous, controllable way of metal doping with nanoparticles, whose shape, size and surface chemistry were regulated. Beyond the thermal analysis, the structural differences between doped and non-doped melting gels were studied.

Overall, the aim of this project was to synthesize gold nanoparticle-doped melting gels and study the interface between the two components of the system, as well as the resulting composite material. Each component of the system has its own characteristic properties such as thermal properties and optical properties that were retained in the new composite material. The goals were to synthesize the hybrid materials and to understand how the two components were affected by this merger.

In more detail, the focus was on the modifications that happened to the nanoparticles after their incorporation in the new medium. In addition, it was important to investigate the structural alterations that occurred after the addition of the gold nanoparticles. Finally, the thermal properties of the composite material were studied, to understand the interactions between the nanoparticles and the melting gels.

The most common precursor used in the preparation of this type of gel is a tetralkoxysilane such as tetraethoxysilane (TEOS) or tetramethoxysilane (TMOS) with four alkoxy groups attached to a silicon atom. By changing the precursors of the sol-gel process it is possible to manipulate the properties of the resulting gels. Properties such as

hardness, porosity and surface area are critical for the development of a coating. Previous studies showed that by introducing organic groups in the silica network, there was a decrease in porosity and surface area.[4] If one or more of the alkoxy groups were substituted by alkyl groups, then the hydrolyzed precursors retain the organic groups in the final gel.

When a combination of mono-substituted and di-substituted alkoxysiloxanes are used for melting gel synthesis, the ratio of the precursors defines the properties of the hybrid silica network. Di-substituted siloxanes are less active molecules and tend to create more linear networks.[5] In this study the precursors used had the same alkyl group, a methyl group. Three different ratios were synthesized with mono-substituted, methyltriethoxysilane (MTES) and di-substituted, dimethyldiethoxysilane (DMDES). The ratios used were 65% MTES – 35% DMDES, 70% MTES – 30% DMDES, 75% MTES -25% DMDES via a sol-gel process, as reported by Klein and Jitianu.[6] The three different ratios of melting gels were modified by the addition of gold nanoparticles. The incorporation was achieved by adding the solution of gold nanospheres during the synthesis process of the melting gel.

Gold nanoparticles are known for their optical properties, biomedical applications like drug delivery or bio-sensing and their surface functionalization among other characteristics and applications. In this study, gold nanoparticles were chosen because their surface can be easily tuned and create a particle with the desirable size, shape and surface functionalization. The nanosphere is one of the most studied shapes, in terms of synthesis and size tuning. The melting gels were doped by gold nanospheres with ~16nm diameter synthesized by a modified Turkevich method.[7]

Hybrid silica glasses have been used for many years for a variety of applications multilayered dielectrics in microelectronics, corrosion resistant barriers and photovoltaic cell applications, to name a few examples. Initially melting gels were developed to replace low temperature melting glasses. Since their discovery, they have been used as corrosion protection coatings on stainless steel, magnesium and titanium alloys. Melting gels have also been used for imprint lithography and ink jet printing in zero-gravity.

A detailed study of doped melting gels and glasses provides valuable information on doping methods and effects of nanoparticles on a hybrid silica network. Briefly, the material was analyzed by UV-Vis spectroscopy for monitoring of the plasmonic properties composite glass, Raman spectroscopy to study its structural fingerprint and FT-IR spectroscopy to monitor the structural evolution of the consolidation process from melting gel to hybrid glass. Transmission electron microscopy was employed to image the hybrid glass and the gold nanoparticles. SAXS was also used to identify the way gold nanoparticles are dispersed in the melting gel. Furthermore, the thermal properties of doped and non-doped melting gels were investigated by DSC, TG-DTA and rotational rheometry. The last one was also used to measure the viscosity of the samples with a range of gold nanosphere concentrations.

The knowledge gained through this project is vital in understanding the way a nanoparticle is incorporated into a hybrid organic-inorganic silica network. This first attempt of doping melting gels with nanoparticles that do not have a protective coating such as PEG or $SiO_2$ showed that no further adjustment of the nanoparticle surface is necessary. The monitoring of the consolidation process with FT-IR spectroscopy clarified how the network is transforming from gel form to glass. Also the comparison among melting gels of different precursor ratios shows why and how the precursor ratio results in

different types of hybrid silica network. Raman spectroscopy revealed that doped hybrid glass samples had well defined peaks whereas non-doped samples gave rise to fluorescence.

Applications such as corrosion protection coatings can use this new composite material and exploit their optical properties. For ease of applying coatings, the viscosity is crucial. It was found that the viscosity can be changed by controlling the concentration of gold nanospheres added during synthesis. Each precursor ratio corresponds to a specific viscosity, glass transition temperature and consolidation temperature, determined by the ratio and the nanoparticle concentration. The information obtained through these analyses helps in applying engineered melting gels with desirable characteristics, in particular, for corrosion prevention coatings.

# Background

Silicon is the eighth most common element on earth by mass. Despite its abundance it is very rare to find in its elemental form. Silicon dioxide and silicates are the most common form to be found in dust, sands and quartz with a variety of crystalline structures. Since silicon is abundant in nature it is a great candidate for the production of new materials limiting the cost, using environmentally friendly materials and preserving rare natural resources. Glass as the first manmade silicon material was produced in Syria dating back in 3000 BC, although hybrid gels have not been recorded to appear for about 5000 years.

*Figure 1: Mayan wall painting of Bonampak, 1600 AD*

The first known sample of hybrid gels dates back in 1600 A.D. where Maya blue pigment was used in wall paintings, Fig. 1, maintaining the vibrant color resistant to corrosion by acids, alkalis and organic solvents. Molecules of natural blue indigo were encapsulated within the channels of clay mineral known as palygorskite. A combination of glass and nanoparticles, like the material studied in this project, was the Lycurgus cup made in the Roman Empire. The glass presents different colors depending on the direction the light is shining relative to the viewer. The different colors are a result of gold and silver nanoparticles contained in the glass. The sol-gel process is a method used to produce

hybrid gels like the Mayan pigment gel. The focus of this study is a nanocomposite gel derived by sol-gel process and modified by gold nanoparticles.

## *Sol-gel process*

According to IUPAC, the sol-gel process is the process through which a network is formed from solution by a progressive change of liquid precursor(s) into a sol, to a gel, and in most cases finally to a dry network.[8] The first sol-gel synthesis of silica from silicon alkoxide was in 1844 by Ebelmen.[9] In this process a colloidal solution (sol) is formed and then through hydrolysis and condensation the sol evolves to a gel-like diphasic system. The liquid and solid phase have a range of morphologies from discrete particles to continuous polymer networks. The next part of the process is the removal of the excess liquid which can be achieved through drying or centrifugation. The solvent removal rate is the determining step for the porous distribution in the gel. The final step of the sol-gel process is the thermal treatment of the gel necessary for further polycondensation of the network, enhancement of the mechanical properties, densification and grain growth. In some cases sintering is used for increase of the structural stability. All of these variations and steps are shown schematically in Fig. 2.

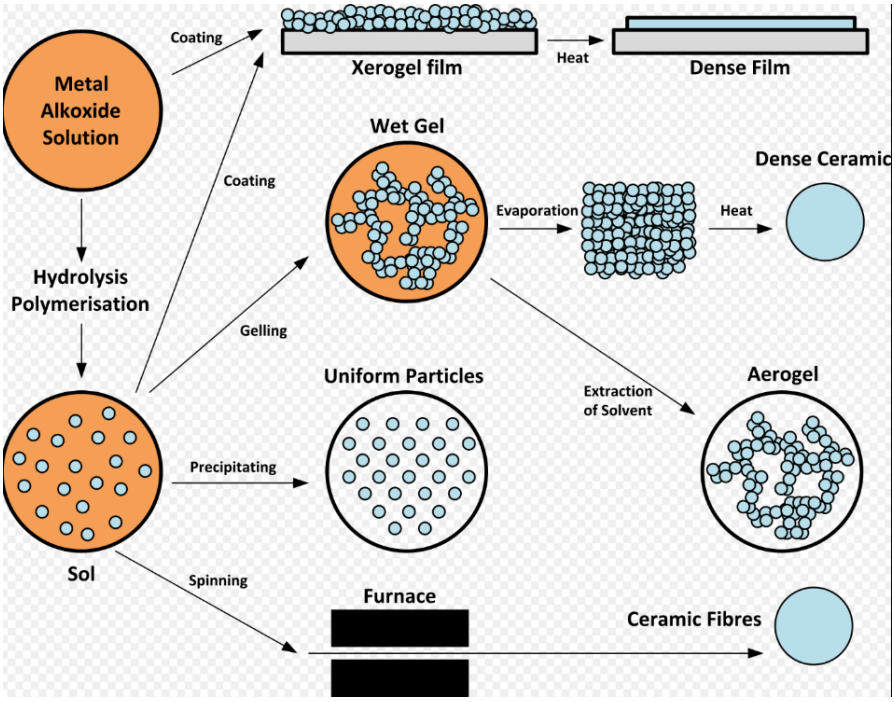


*Figure 2: Schematic used by Chemat, Inc. to show versatility of the sol-gel process, starting from metal alkoxide solutions.*

This type of synthesis method is controlled by the precursors, their ratios, the chosen catalyst, the water ratio and the solvent. [10] All of these parameters can create countless results and materials.

A desire to combine properties of different materials at a molecular level has led to the creation of ORMOSILs (Organically Modified Silicates). A sol-gel process combining organo-substituted silicon esters creates a hybrid organic-inorganic network called ORMOSILs. Soluble reactive monomers are required for the sol-gel synthesis of organic-inorganic polymers.[1] Mixing several monomers in a mutual solvent presents an easy route to facilitate hydrolysis and condensation reactions that are necessary to carry out the sol-gel synthesis process.

## *Hydrolysis and Condensation*

Hydrolysis is the first type of reaction in the sol-gel process, which replaces alkoxide groups (-OR) with hydroxyl groups (-OH). Once some precursor molecules are hydrolyzed the second type of reaction starts. This reaction is condensation, which produces bridging oxygen bonds (Si-O-Si) and by products water and alcohol (ROH) from the condensation of silanols. The hydrolysis rate depends on the sol-gel precursors, but the duration of the hydrolysis step is short and it contributes very little to the gelation time. Steric hindrance can decrease the rate of the hydrolysis mechanism. The second step, condensation, starts as soon as an alkoxy group has been hydrolyzed. At the beginning of condensation, linear chains are created. When partial polymerization has occurred, further condensation occurs only through the crosslinking of linear chains. Ultimately, the three dimensional network is formed through further crosslinking of the linear chains, which are separated by alcohol and water molecules.[11] These reactions are shown sequentially in Figure 3[12].

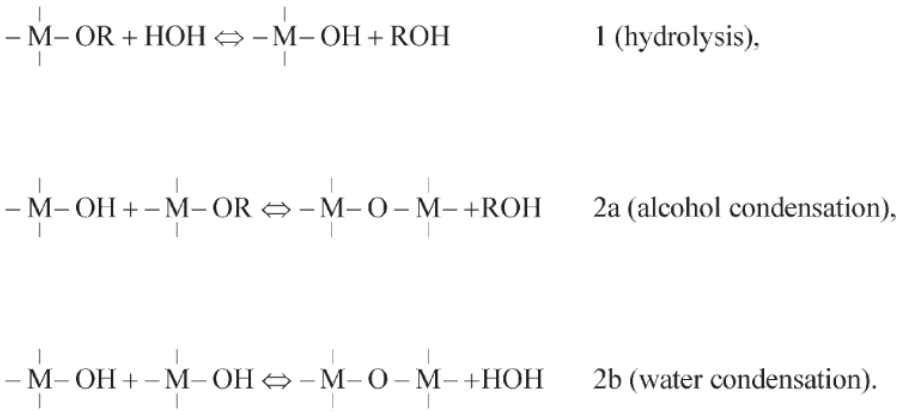


*Figure 3: Reactions that take place during the sol-gel process.*

When the sol-gel process is used to apply coatings, the coating is formed directly from the sol, which is applied to a substrate. The coating is applied by dipping the substrate into the solution, pouring the solution or the substrate or spraying the solution onto the substrate.

In order to control the thickness of the coating, the organic functionality of the silicon atom is important. Hybrid films have been prepared using MTES-TEOS, PhTES-TEOS and MTMS-TMOS. For example, methyl-substituted melting gels were used as corrosion protection layers on AISI 304 stainless steel. In this study melting gels were stable surface films that protected stainless steel effectively from NaCl solution.[3] Phenyl-substituted melting gels were also used as corrosion protection layers for lithium metal, and the solvent ratio was tuned for optimal thickness of the crack-free coatings.[13] Barrier coatings against water vapor and gases confirmed the sealing properties of organic-inorganic hybrid gels. The organic component bonded in the silica network provides flexibility, decreases the processing temperatures and reduces the porosity.[14]

## *Precursors*

It is known that the rates of hydrolysis and condensation of the precursors used during synthesis predict the physical properties, like surface area, porosity, wettability, pore volume and size. To further manipulate the properties, there are two methods to introduce organic groups into the silica network, either through co-condensation of precursors with organic groups or through post-synthesis grafting. Although the post-synthesis grafting method starts with well-defined and structurally ordered materials, the resulting material has an inhomogeneous distribution of organic groups.

The precursors used to create most ORMOSILs are organosilanes which have four atoms attached to a silicon atom. The structures of silicon compounds use as precursors can be described by the general formulas $R_n$'- $Si(OR)_{4-n}$ when one, two, three or four oxygen atoms are attached to the silicon atom. In the case of co-condensation, the synthesis method with the functionalized precursors creates a more homogeneous distribution of the organic groups. Precursors used for the sol-gel synthesis of hybrid organic-inorganic gels are organofunctional molecules that have epoxy, acrylic, alkyl, allyl, phenyl and amino-functional substitution. Different organic groups are used to alter the coatings and their properties. For example, an amino-containing coating may exhibit good adhesion, but its corrosion protection is not as effective due to low hydrolytic stability.[15]

*Table 1: Methyl- and Phenyl-substituted precursors containing methoxy groups.*

| Precursor | Chemical Formula | Molecular Weight | %$SiO_2$ | Number of Reactive Groups |
|---|---|---|---|---|
| Tetramethoxysilane | $C_4H_{12}O_4Si$ | 152.22 | 39.5 | 4 |
| Methyltrimethoxysilane | $C_4H_{12}O_3Si$ | 136.22 | 44.1 | 3 |
| Dimethyldimethoxysilane | $C_4H_{12}O_2Si$ | 120.22 | 50.00 | 2 |
| Phenyltriemethoxysilane | $C_9H_{14}O_3Si$ | 198.29 | 30.3 | 3 |
| Diphenyldimethoxysilane | $C14H16O_2Si$ | 244.36 | 24.6 | 2 |

Some common precursors containing methoxy groups are listed in Table 1, with their chemical formula, molecular weight, oxide content and number of reactive groups. The

corresponding precursors containing ethoxy groups are listed in Table 2. The most frequently used materials for preparation of silica gels are tetraethoxysilane (TEOS) and tetramethoxysilane (TMOS). Gelation time increases with more carbon atoms attached to the silicon atom of the precursor according to Park et. al.[16] The steric hindrance is also reported to affect the crosslinking. Photocurable ORMOSILs can be produced by organosilanes with methacryl, vinyl, allyl groups.

Table 2: Methyl- and Phenyl-substituted precursors containing ethoxy groups.

| Precursor | Chemical Formula | Molecular Weight | %SiO2 | Number of Reactive Groups |
|---|---|---|---|---|
| Tetraethoxysilane | $C_8H_{20}O_4Si$ | 208.33 | 40.5 | 4 |
| Methyltriethoxysilane | $C_7H_{18}O_3Si$ | 178.30 | 33.7 | 3 |
| Dimethyldiethoxysilane | $C_6H_{16}O_2Si$ | 148.28 | 40.5 | 2 |
| Phenyltrieethoxysilane | $C_{12}H_{20}O_3Si$ | 240.37 | 25.0 | 3 |
| Diphenyldiethoxysilane | $C_{16}H_{20}O_2Si$ | 277.42 | 22.1 | 2 |

Dimethyl diethoxysilane (DMDES) derived mesoporous silicates are found to have increased specific area and decreased pore volume with the increase of di-substituted precursor.[17] Methyl-substituted precursors need less time to gel than ethoxy, due to steric hindrance.[18]

The degree of substitution determines the surface area of the hybrid gels. Higher mono-substituted content leads to higher surface area, as was shown by the comparison of TMOS-MTMS and TEOS-MTES gels.[18] Mono-substituted alkoxides, when they are

combined with di-substituted alkoxides, act as bridges between hydrolyzed precursor molecules, creating a 3-dimensional network. As DMDES content increases, the number of unhydrolyzed Si-C bonds increases. The reduction of hydrolyzed groups allows fewer bridging oxygens or crosslinks between the silica chains. All the above mean that with the increase of DMDES, there is a more linear network.

## *Solvents*

The main role of solvents is to prevent liquid-liquid phase separation of water and alkoxides and to control kinetics of the reactions that are governed by the concentrations of silicate and water. Solvents used in the sol-gel process can be classified based on polarity -- as polar and non-polar -- and based on the labile proton -- as protic and aprotic. Based on the polarity of the species at the beginning or during hydrolysis the appropriate solvent is chosen. Solvents also affect the formation of the hybrid silica network. For more polar tetrafunctional silicate species in water, alcohol and, in general, more polar solvents are used. In alkyl-substituted or incompletely hydrolyzed systems, solvents like tetrahydrofuran are used. Ether alcohols that exhibit both polar and non-polar character are used for solutions that have both polar and non-polar species.

Many properties of the solvents influence physical properties of the gels. For example, the size of solvent molecules affects the surface area. The easier the evaporation of the solvents is during the sol-gel process, the higher the surface area is. Dipole moment is another important characteristic especially for electrostatically stabilized systems. This is because of the attraction or repulsion of charged catalytic

species such as $OH^-$ and $H_3O^+$ from potential reaction sites. Lastly, the availability of labile protons determines how strongly anions or cations are solvated through hydrogen bonds.

Alcohol is used as a solvent because water and alkoxysilanes are both miscible in it. When sol-gel solutions are mixed without added solvent, especially under acid conditions, some alcohol is present, since it is produced during hydrolysis of alkoxides. The alcohol produced from the reaction is sufficient to homogenize the immiscible phases in a solution.

## *pH*

The network formation is governed by the pH of the solution during condensation/polymerization reactions. The pH is divided in three regions of interest for the polymerization reaction, <pH 2, pH 2-7 and >pH 7. The regions are split based on the

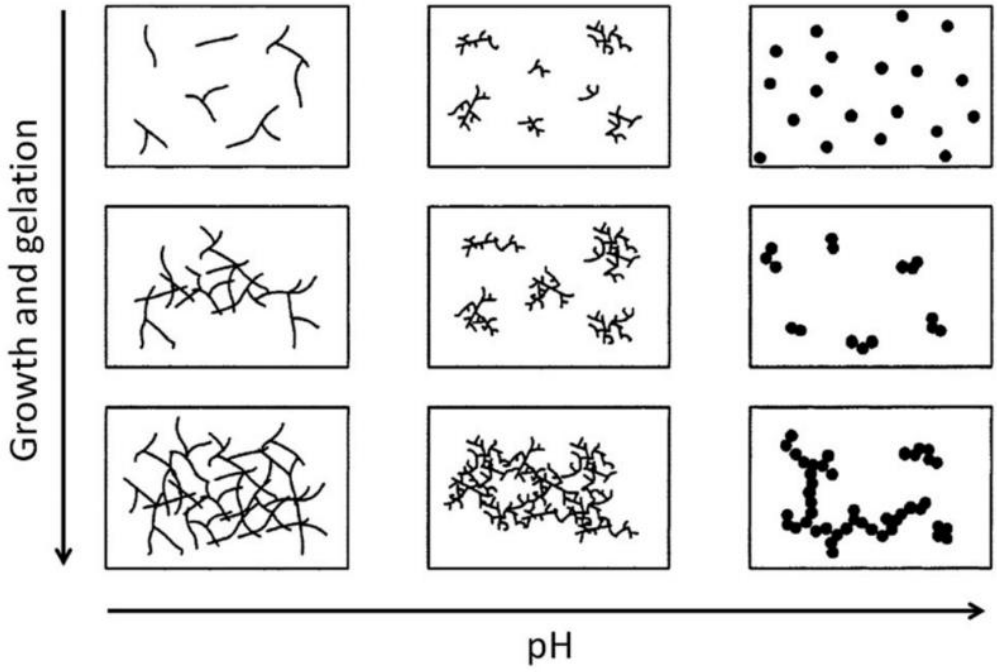


*Figure 4: Diagram showing the effect of pH on the structure and growth of gels derived from sol-gel process.*

point of zero charge (PZC), the isoelectric point (IEP), and the solubility and dissolution rates of silica. Lower pH results in linear species, whereas higher pH creates highly condensed networks. The condensation reaction is dependent on the concentration of hydroxyls.

Figure 4 shows schematically what the gelling process involves. The pH is increasing from left to right, and the time is increasing from top to bottom. For pH 2-7 condensation occurs slowly between highly condensed (acidic) species and less highly condensed neutral species. The formation rate of the dimers is slow, but once dimers are formed, they react with monomers forming trimers which form tetramers when reacting with monomers. Near the IEP where there is no electrostatic particle-particle repulsion, growth and aggregation occur simultaneously. Because of the low solubility of $SiO_2$ at this pH growth stops when particles reach 2-4nm.

In the case of condensation above pH 7, highly condensed species are more likely to be ionized, hence mutually repulsive. At this range of pH, growth occurs by the addition of monomers to more highly condensed particles. Further growth of the primary particles advances by Ostwald ripening. The growth rate depends on the particle size of small particles and deposition of soluble silica on larger particles.

In the sol-gel process, catalysts influence not only the rate of the reactions but also the morphology of the network.[19] As shown in Figure 4, the pH affects the way in which a sol-gel synthesis progresses. Low pH creates more linear networks and less condensed materials, whereas high pH creates more closely packed materials that can form particles.[20] In Table 3 there is a summary of the effects of each catalyst according to Pope.[21]

*Table 3: Effects of Catalyst in the Sol-Gel Process*

| System | Catalyst | Effects |
|---|---|---|
| Silica | HCl | Slow hydrolysis relative to the condensation reaction, small pores, High bulk density |
| Silica | $NH_4OH$ | Rapid hydrolysis compared to the condensation reactions, large pores, low bulk density, spherical particles |
| Silica | $NH_4Cl$ | "Postponed" hydrolysis followed by rapid gelation |

Acid catalysis has been shown to create surfaces with lower roughness than base-catalysis. Silica thin films have Si-O-Si peaks identified by FT-IR spectroscopy. Those peaks are a result of condensation of silanol groups creating coarse particles. Base catalyzed coatings, on the other hand, have better optical properties.[22] Due to the fast hydrolysis rate, the condensation reaction is the reaction that controls the overall rate of the sol-gel process. For acidic hydrolysis, the condensation rate is expressed by a logarithm of time.[23] The methyl groups decrease the condensation time because they reduce the net charge on the silicon atom which is the key parameter for nucleophilic condensation processes above the isoelectric point.[24]

## *Water to Precursor Molar Ratio*

Water-to-alkoxy molar ratio (r) has been widely studied for the effect it has on the formation of the network. High values of r are expected to promote the hydrolysis reaction and result in fully hydrolyzed monomers before condensation has advanced.

The hydrolysis of the monomers affects the rates of alcohol and water produced during the reactions. When $r \leq 2$, the alcohol-producing reaction is favored and the reaction is considered partially hydrolyzed. When $r \geq 2$ the water-forming condensation reaction is favored and the solution is considered fully hydrolyzed.

## *Organically Modified Silicates (ORMOSILs)*

Depending on the kind of molecular bonds or interactions in the hybrid network ORMOSILs are divided in two classes: Class I hybrids and Class II hybrids. In Class I, the interface of the organic and inorganic components is based on van der Waals forces, hydrogen bonds and electrostatic forces. Class II, on the other hand, represents materials where the organic and inorganic components are linked through strong, covalent or iono-covalent bonds.[25] Since there are many combinations of materials, hundreds of hybrid materials have been developed by sol-gel processes. Utilization of different precursors has led to a variety of products with properties associated with glass and with polymeric materials.

Functional hybrid organic-inorganic nanocomposites have been used in a variety of applications over the years. With respect to the optical properties of hybrid glasses, such as emission, absorption, non-linear optical and sensing, these materials are designed for use in many optical applications. For example, hybrid sol-gel derived matrices have been used in solid state dye lasers because of their longer lifetimes and high repetition rates.[26-28] Organic-inorganic silicates with absorption properties can also be used for optical switches, energy conservation coatings, and display coatings such as organic light-emitting diode (OLED). The interface between non-linear optical dyes

and hybrid materials can produce systems that block intense light irradiation of lasers, protecting sensors and cameras.[28, 29]

Sanchez in a detailed review of applications of ORMOSILs gathered the numerous ways these types of silicates are used in a variety of fields. The research areas that have used ORMOSILs in non-linear optical applications include a new matrix that can be used as a host for a plethora of materials. Hybrid organic-inorganic gels and glasses can host metallic or polymer nanoparticles, carbon dots, fullerenes and graphene oxides.[30-33] Entrapment of species in ORMOSILs has been used for several years as a method of sensor development. Some of the species that can be entrapped are antigens, antibodies, enzymes, proteins, optical probes and redox probes.[34, 35] Also, sol-gel derived silicate networks can be used as sensors, such as optical oxygen sensors, prepared by doping xerogels with luminophore molecules.

In another case, Wu et. al used ORMOSILs as an entrapment matrix for Ag/AgCl antibacterial materials. Instead of using quaternary ammonium salts, which are widely used in cationic disinfectant coatings, they created a new insoluble cationic polymer coating. This coating could exhibit antimicrobial behavior through contact with water without requiring the release of reactive agents. [36]

Another application of hydrophobic ORMOSILs is antireflective coatings. Hybrid silica films made with PTES and TEOS have been used as antireflective coatings as a double layer. These coatings have transmittance percentages from 98.7% to 99.3% depending on wavelength range. [37] Protective- antireflective coatings offer UV-protection from light induced damage caused by photons. Undoubtedly protection from UV light is necessary for organic compounds, and wooden or plastic surfaces.

Antifouling coatings are required for surfaces that are immersed in the sea. Water vehicles, even bridges, which have exposed surfaces to water are susceptible to vegetation growth. The low surface energy and hydrophobic properties of antifouling coatings act as inhibitors to vegetation growth.[38]

The need for surface protection is essential in corrosion protection. Epoxy-silica coatings, which bond chemically with Fe-OH formed when iron surfaces oxidize, provide corrosion protection.[39] Surfaces prone to abrasions and scratching like polycarbonates have immediate need of scratch-resistant coatings. ORMOSIL sols of diethylenetriamine-TMOS have provided scratch protective for highly transparent coatings.[40] The list of applications of ORMOSILs could go on, but the examples given are a good representation of their positive contributions.

## *Vibrational Spectroscopies*

Fourier transform infrared (FT-IR) and Raman spectroscopies are both vibrational spectroscopies used to study the structure of a compound. Both spectroscopies decipher the way a material is formed, giving complementary information. IR spectroscopy depends on differences of dipole moment, while Raman spectroscopy relies on a change in polarizability of a molecule.

The majority of ORMOSILs have a complex network comprised by Si, C, H, O atoms that are bonded according to the synthesis method that was used. These elements are the backbone of the hybrid organic-inorganic network and with the addition of modifiers or dopants create a wide range of materials.

In order to understand the structure of these materials FT-IR is usually employed for the structural analysis of the hybrid network. In FT-IR, the light absorption in the infrared part of the spectrum causes specific vibrational modes that are unique to each molecular structure. The fundamental structural unit of pure silica gel is the tetrahedral $SiO_4$ that has one silicon atom bonded with four oxygen atoms. The 3-dimensional network of an ORMOSIL carries corner-sharing tetrahedral units which are arranged in cyclic siloxane structures. Non-bridging bonds, small ring and peroxide bridges are considered defects although they are structurally stable. Apart from pores that have hydroxyl groups on their surface, there are other inhomogeneities introduced during the sol-gel process.

There are several studies that investigate the formation of structural siloxane rings during hydrolysis and condensation reactions.[41, 42] TEOS as the most common precursor for the preparation of ORMOSILs has been widely studied. Hydrolysis of TEOS creates siloxane oligomers consisting of 4-fold siloxane rings that are maintained in the network during condensation reactions. Hench et al. using a quantum calculation studied which species are energetically more favorable during polymerization. The study showed that cyclic siloxane tetramers are preferred more than chains, although 6-fold rings are less strained and more kinetically favorable. In Figure 5[43] are shown the two types of rings found in this type of network.

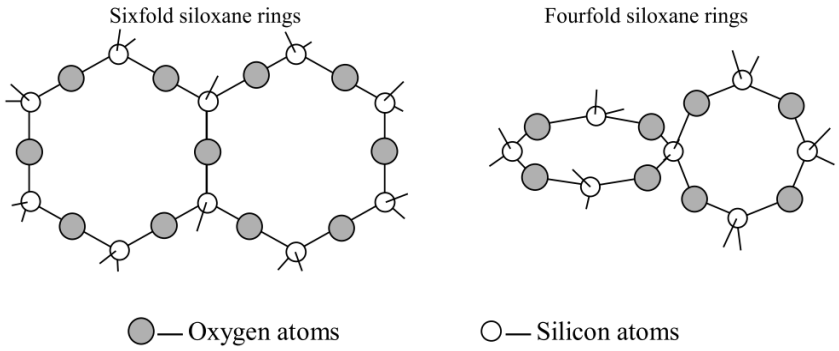


*Figure 5: Schematic representation of 6-fold and 4-fold siloxane rings.*

Even though FT-IR has been used to study the structure of a hybrid organic-inorganic network the information is limited. Often the interpretation of the spectra is not able to clearly identify the structural and compositional properties of both parts of the network. A major problem is caused in a specific region of the spectrum 900-1400 $cm^{-1}$ where many vibrations have overlapping peaks. In an effort to quantify the observations of that region Fidalgo performed a deconvolution of the spectra of pure silica and hybrid films preserving the number of the peaks and their positions. However, the studies cover only the hydrolysis and condensation parts of sol-gel process. The heat treatment of gels and their transition to glass-like materials needs further investigation.

Raman spectroscopy involves using light at a specific wavelength that interacts with molecular vibrations, phonons or other types of excitations in the system. The result is a shift of the laser phonons, which corresponds to a spectrum carrying information of the vibrational modes of the system. Raman is not used as often as FT-IR of the vibrational spectroscopies for the structural studies of ORMOSILs because of the low level of useful Raman signals. Strong interfering signals caused by laser-induced fluorescence of the organic part of ORMOSILs makes the collection of spectra a difficult task. However, by

using the correct optics and configurations fluorescence signals can be decreased or eliminated.[44]

The evolution of hydrolysis and condensation reactions was monitored by de Ferri et al. using Raman spectroscopy. Throughout this experiment the changes of the hybrid silica network were recorded by Raman. During hydrolysis the disappearance of Si-alkoxide $CH_2$ was noticed along with the increase of the hydrolyzed alkyl-silane peak. Condensation led to the formation of the silica network and the rise of the Si-O-Si symmetric bending and stretching.[45] Methyl concentrated on the surface as was recorded by Raman. A higher amount of organic groups increases the hydrophobicity of the films. [18]

An increased degree of crosslinking causes an upward shift in the Si-O-Si $V_{sym}$ and $v_{asym}$ . The vibrational asymmetric peak withstands more of a shift than the symmetric because of the lattice compression due to densification. The redistribution of O, C atoms is found to lead to a change in the macroscopic porosity. Higher wavenumbers have also been correlated with the increase of Si-O-Si bridging angle.

The data obtained by Raman are complementary to data obtained by FT-IR or NMR, making them useful for the combined analysis of the complex organic-inorganic structure. [46, 47] The lack of strong signals is exploited in the development of surface enhanced Raman spectroscopy substrates, which will be discussed further in the applications part.[48]

## *Doped ORMOSILs and Applications*

Composite materials with plasmonic nanoparticles have been synthesized in two ways. First, the nanoparticles have been synthesized in situ by chemical, thermal or photoinduced reduction. The second way is to introduce the nanoparticles as a colloidal suspension, which is the route followed in this project. ORMOSIL gel glasses have been used as nanoparticle hosts because they are made at low temperatures, the have low porosity, and they are flexible and elastic. Their high hydrolytic and thermal stability makes them an ideal host for molecules and nanomaterials.

A few of the many examples of gels used as hosts are listed here. Silica glasses with dispersed semiconductor or metal colloid particles are used in optical devices due to their high non-linear optical properties. [49] Sol-gel derived self-assembled monolayers (SAM) synthesized with mercaptopropyltrimethoxysilane can act as host matrices for gold nanoparticles. The SAM layer containing thiol functional groups is present to promote the self-assembly of gold nanonoparticles into the silicate network. Also, modified silicate films have been used as nanoscale electrodes with a gold substrate. [50]

In some studies, the surface of the gold nanoparticles are coated by a silica layer to provide more stable nanoparticles. Nanocomposite metal-doped glass are designed to be used as optical limiters against tunable laser.[30] ORMOSIL-gels containing gold particles have been used as SERS substrates. In one case, the gold particles where synthesized in the silica monoliths using photodeposition. The SERS activity of the doped substrate was used for the successful detection of pyrazine, but the study reported a high level of inhomogeneity in the size distribution of the particles.[51]

In an advance in the incorporation of gold nanoparticles in gels, Lunden et al. created a gold doped hybrid silica glass that allowed self-orientation to the gold bipyramids that were used as a dopant. Gold nanospheres and bipyramids with silica coatings were dispersed in the gels and had a preferred orientation that did not affect the optical limiting properties of the material. Optical limiting was confirmed at 532nm but not 600nm. [52] Lunden et al. also used doped monolithic silica sol-gel glasses for reverse saturable absorption. The glasses were doped with platinum acetylide complexes containing four or six phenylacetylane units. The high optical quality glasses were also doped with spherical and bipyramidal gold nanoparticles.[53] An in situ method of doping was developed by Pal by mixing Au and Ag ions in sol-gel silica matrices. Through UV and thermal annealing Au-Ag alloy nanoparticles were formed with a homogeneous size distribution. [54]

In another application according to Santana et al., sol-gel coatings were doped with clay nanoparticles for corrosion protection. A combination of cerium and clay nanoparticles give self-healing and barrier properties to the coating respectively. The composite material showed significant improvement of the anticorrosive behavior of coating under immersion tests.[55] Gold nanoparticles were used to modify ORMOSIL gel glass to provide non-linear optical properties to it. The addition method of the nanoparticles was solvent-assisted dispersion which is the same method used in this project.

## *Nanoparticles*

Plasmonic materials and their light-matter interactions have been the center of attention since 1990, when there was an exponential growth of nanotechnology research. Particles that have at least one dimension in the range of 2-100nm are called nanoparticles. On this size scale, the properties of the material depend on its size and shape. Due to the lack of symmetry at the interface or to electron confinement, new properties develop that do not scale linearly with size. At the nanometer scale, the collection of atoms or molecules does not have the properties of the bulk material or its individual constituents. The size and shape of the nanoparticle plays a more important role in its properties than the type of material, meaning nanoparticles with different properties can be produced from the same material.

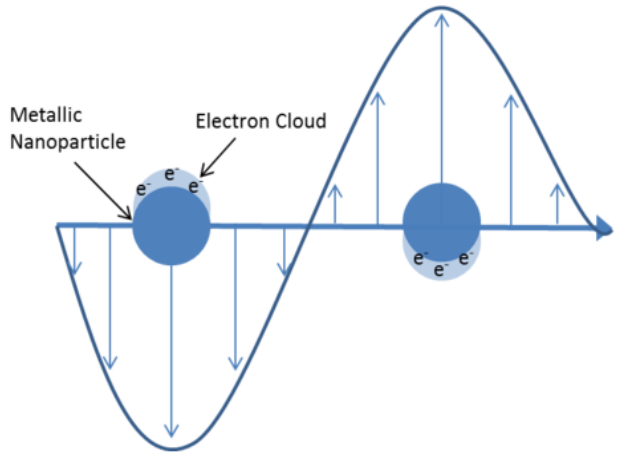


*Figure 6: Schematic showing surface plasmon resonance for metallic sphere*

Noble metal nanoparticles that have free electrons on their surface that can be excited by a light source that has a wavelength much bigger than their size. When nanoparticles are under these circumstances, their free electron cloud is oscillating collectively. This phenomenon is called Localized Surface Plasmon Resonance (LSPR). The easiest way to observe this phenomenon is by UV-Visible and sometimes Near Infrared spectroscopy, which show an absorbance at specific wavelengths, because as the size and shape changes the color of the solution changes due to LSPR. The

wavelength where the absorbance is recorded depends on the characteristics of the nanoparticle. A schematic showing a plasmon resonance of a gold nanospheres is shown in Figure 6 with the corresponding absorbance spectra. The absorbance spectra are characteristic of the materials that constitute the nanoparticles, their size, shape and surface functionalization. Some properties of nanoparticles that are noteworthy are electromagnetic field enhancement and thermal effects, both in small distance from the nanoparticles. The plasmon resonance absorption has an absorption coefficient that is orders of magnitude higher than Rhodamine B which is an efficient absorber.

Gold and silver nanoparticles have been investigated in great detail regarding their chemistry, synthesis protocols and surface functionalization. Many studies have been conducted on a wide range of shapes and sizes, thus creating a substantial database of how to tune them for the desired properties of a nanoparticle. The

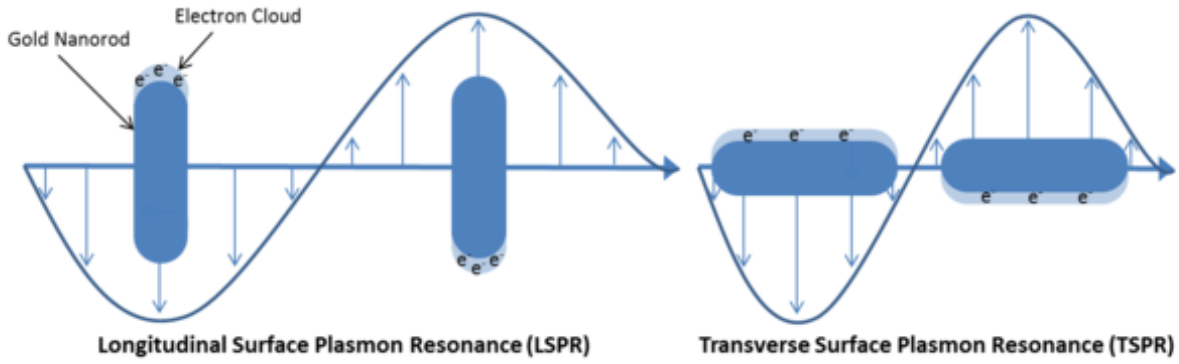


*Figure 7: Schematic showing of the two SPRs of gold nanorods.*

introduction of anisotropy in shapes creates stronger absorption resonances, which is useful in sensitive detection applications. Nanorods have attracted the attention of researchers because there are many synthetic protocols that can control their aspect ratio which in turn controls their optical properties. Nanorods as shown in Figure 7 have two plasmon resonances one due to the longitudinal and one due to the transverse

oscillation. The resulting absorbance spectra of a gold nanorod is depicted in Figure 7 where two peaks can be distinguished. More complex geometries like nanostars have been studied extensively for the propagation of surface plasmons. Tsoulos investigated the contribution of tips and spikes of gold nanostars as discrete units alongside with the effect of nanoparticle orientation to coupling mechanisms.[56]

There are two approaches to the synthesis of nanoparticles one is called "bottom up" where the nanostructures are formed from atoms that come from an ion reduction. The other approach is called "top down" where material is removed from the bulk material until the morphology of the desired nanostructure is achieved. Surface modification of metallic nanoparticles can be achieved with thiolated silicon polymers. The modified nanoparticles can be easily introduced in sol-gel matrices. [57, 58]

## *Synthesis Methods of Gold Nanoparticles*

Growth of gold nanocrystals in aqueous solution was described by Faraday in 1857.[59] The development of a simple synthesis method of gold nanoparticle was discovered by Turkevich in 1951. The synthesis protocol requires only three ingredients chloroauric acid, water and sodium citrate.[60] Since Turkevich, who developed one of the most popular approaches for the synthesis of gold nanoparticles, many other protocols have been developed. Based on that synthesis protocol, Frens was able to control the size of the nanoparticles by varying the ratio of gold salt to sodium citrate.[61] Sodium citrate concentration used during gold nanoparticle synthesis has more influence as a pH mediator than as a reducing agent. A series of three possible equations for the citrate capping reaction are given in Figure 8, with their respective reaction constants.

Figure 9 shows a schematic of the synthesis process starting with chloroauric acid and sodium citrate. The gold nanoparticle is capped by the citrate groups.

$$H_3Cit \rightleftharpoons H_2Cit^- + H^+ \quad K_{a1} = 7.10 \times 10^{-4}$$
$$H_2Cit^- \rightleftharpoons HCit^{2-} + H^+ \quad K_{a2} = 1.68 \times 10^{-5}$$
$$HCit^{2-} \rightleftharpoons Cit^{3-} + H^+ \quad K_{a1} = 6.40 \times 10^{-6}$$

*Figure 8: Equilibrium equations of citrate*

According to Ji there are two different pathways for the formation of gold nanocrystals depending on the pH of the solution. The formation could occur through a nucleation-growth pathway or a nucleation-aggregation-smoothing pathway, the determining point of the followed pathway is at pH around 6.2-6.5.[62] The gold

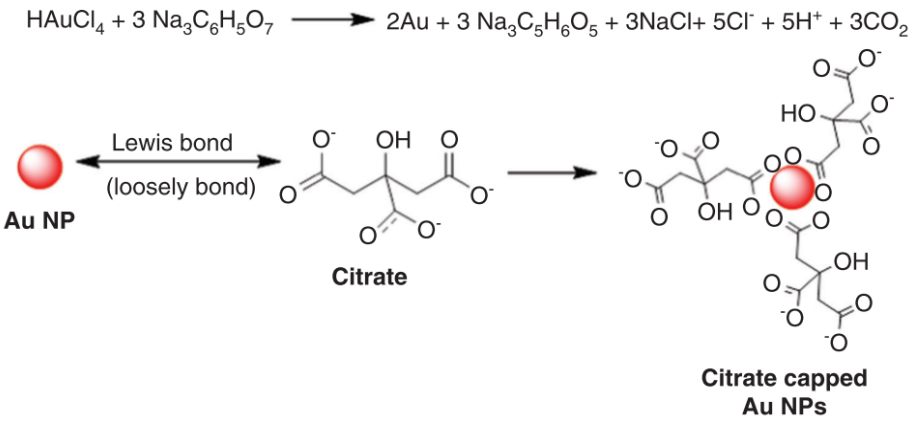


*Figure 9: Gold nanosphere synthesis reaction according to Turkevich method of sodium citrate reduction.*

nanospheres used in this study were synthesized according to a modified Turkevich method that creates nanoparticles with 16nm diameter.[63]

Synthesis of oxide nanoparticles during the sol-gel process can provide chemical bonds between the matrix and the nanoparticles. The preparation of Au, Ag and Pd

nanoparticles reported by Pandey et al. exploited functionalities of glycidoxy- and amino groups of alkoxysilanes.[64] Silver nanoparticles have been synthesizes in situ in ORMOSILs although the size distribution was non-homogeneous. One of the disadvantages of in situ nanoparticle synthesis is the size and shape discrepancies as confirmed by Reinsfield.[65]

## *Applications of Nanoparticles*

The optical properties of noble metal nanoparticles have fascinated scientists because of the numerous applications that they have. The development of nanomaterials carrying non-linear optical materials gave rise to the development of nano-scale optoelectronics and photonic devices. Metal nanoparticles have a wide range of applications that take advantage of the large third order non-linearity. Zhu developed carbon nanotubes doped with ZnO nanoparticles. The system demonstrated an ultrafast nonlinear optical switching behavior and large saturable absorption opening the possibility to be used for saturable absorber devices.[66] Gold nanoparticle and nanoclusters have been found to exhibit strong optical limiting for both nanosecond and picosecond laser pulses. The optical limiting performance has a correlation with the size of the nanoparticle and it is attributed to nonlinear scattering.[67] Wang et. al showed that aggregates of gold nanoparticles had enhanced optical limiting and were governed by the electrolytes that were used. Aggregates formed by higher concentration of electrolyte resulted in better optical limiting performance.[68]

Electromagnetic energy transport along copper nanoparticles was investigated by Maier in three different arrays. It was proven both with experiments and simulations that closely spaced nanoparticles facilitated the propagation of electromagnetic waves

by near field coupling.[69] A variety of silica coated particles derived from epoxysilane and bisphenol A have been introduced into hybrid matrices. In one study $Al_2O_3$, $ZrO_2$ and SiC nanoparticles were added to hybrid organic-inorganic matrices. For further stabilization of the nanoparticles, a surface modification with Si-OH groups was performed. AlOOH particles were introduced into the matrix without any modification. [11]

Knowing that the physical phenomenon behind Raman spectroscopy is the inelastic scattering of photons by a molecule having quantized vibrational level/signature, Raman scattering has an inherent limitation due to the low scattering intensity of the molecules. However, in the presence of plasmonic species or rough metal surfaces, Raman scattering intensity can be enhanced up to $10^{14}$ orders of magnitude.[70] Surface Enhanced Raman Spectroscopy (SERS) sensors have been used for the detection of organic molecules, oligonucleotides and proteins.[71] A biosensor with a single cell detection ability was developed using gold nanostars for SERS. Utilizing the enhanced signal provided from the nanostars the biosensor successfully detected and quantified the expression of a cancer cell biomarker.[72]

## *Melting Gels*

A subcategory of Class II organically modified silicates that has strong covalent bonds in its network is so-called melting gels. Melting gels got their name because of their unique property to change viscosity according to the temperature of the material. They soften at a certain temperature, called the melting temperature. This softening behavior however is not melting in a thermodynamic sense.[73] After the synthesis of melting gels, the hybrid silica network maintains some unhydrolyzed groups. When the

melting gels are held isothermally at the consolidation temperature, the mostly linear chains are more flexible and are allowed to come closer into a position that favors hydrolysis condensation reactions between the chains. This crosslinking process is permanent and prevents melting gels from resoftening.

The transition from gel to rigid hybrid raises the question about what structures exist in the gel at that time. For mixtures of precursors with two reactive groups and one reactive group, the simplest structures that will form are dimers, tetramers and silesquioxanses.[74] Hypothesizing that melting gels contain mostly chains that can move when heated above the softening temperature, the chains are flexible up to their consolidation temperature. By increasing the temperature the chains can move to a favorable position that allows them to react further through condensation reactions of the hydrolyzed ends of the chains. The final condensation reactions create a denser, cross-linked network which is the final product of the melting gel synthesis, a hybrid glass.

Freshly prepared melting gels and unconsolidated melting gels exhibit glass transition behavior, where areas of the network exhibit relaxation phenomena like polymer nanocomposites. Using Differential Scanning Calorimetry and Rotational Rheometry, the glass transition temperatures of the melting gels have been identified. The glass transition temperature is correlated with viscosity, dielectric constant and mechanical properties and reflects the degree of cross-linking in the silica network. As the number of oxygen bridges between silicon atoms increases, the glass transition temperature should also be increasing.

In previous studies, FT-IR spectra collected from melting gels during heating and isothermal treatment were used to follow the chemical, hence structural evolution of the gels. Only $CO_2$ was identified in the evolved gasses during the consolidation process.

The fact that $CO_2$ was emitted during this process indicates the decomposition of unreacted organic groups. Also, during the consolidation no water was identified in the evolved gasses.[75]

## *Glass Transition Behavior and Thermal Analysis*

Slow or static methods have been used to measure the glass transition temperature of materials. Differential Scanning Calorimetry (DSC) and Differential Thermal Analysis are widely used to identify the glass transition temperature. With simple extrapolative corrections, by measuring the changes in specific heat of the material at the liquid-glass transition, the glass transition temperature is read directly from the differential scanning calorimeter plot of specific heat versus temperature.[76]

DSC is a type of thermal analysis that measures the amount of heat required to increase the temperature of a sample, comparing it to the heat of a reference material, as a function of temperature.[77] The glass transition temperature $T_g$ is not strictly a particular temperature. Instead, it refers to a temperature range where a soft material transforms to a rigid, glassy material. The transition often is measured in terms of stiffness or modulus.

Differential Thermal Analysis (DTA) is an analysis method that is used to monitor the thermal properties of a material. This technique measures the temperature difference between the sample and a reference material during heating at a constant rate. The DTA measurement records any exothermic or endothermic reactions that occur during heating.

Another thermoanalytical technique is Thermogravimetric Analysis (TGA). The apparatus that is used for this analysis is a combination of a microbalance with a furnace and a temperature controller. While heating a material, the mass of the sample is measured. This analysis is used to monitor the thermal decomposition and then to calculate the amount of inorganic and organic or volatile components.

When this technique was used before to study methyl-containing melting gels made with DMDES and MTES, weight loss percentage increased as the DMDES ratio increased. The weight loss occurred in two steps. The first step one was due to the removal of ethoxy and hydroxyl groups. The second step was due to the combustion of methyl groups. A broad exothermic peak indicated a uniform distribution of methyl-groups throughout the silica network, while a narrow peak indicated that methyl- groups had a higher concentration on the surface of the gel.[78] DTA also showed an exothermic peak that confirmed the combustion of methyl groups identified by TGA.[18]

In another study, thin film barriers were made from precursors of different levels of substitution groups. The thermal analysis showed that the alkyl group did not affect the endothermic process of removing solvent or water. However, precursors with large substituted groups required higher temperature to remove the bulkier groups, such as phenyl-groups. The alkyl group caused a decrease in the temperature of the exothermic peak as the size of the group reduced. MTES with TEOS samples showed that the methyl group is easier to remove than the ethoxy-groups during DSC measurements.[18]

As expected, the higher organic content increases the weight loss of a sample, because organic matter is susceptible to thermal decomposition. The consolidation temperature is dictated by the degree of crosslinking of the hybrid silica network.[79] Consolidation temperatures of melting gels are listed in Table 4, reported by Jitianu. A

decrease in the di-substituted precursor leads to a decrease of the consolidation temperature. Di-substituted alkoxides have only two ethoxy- groups available to create bonds with the silica network. DMDES without MTES remains liquid throughout the sol-gel process because the linear chains do not have the bonds needed to create a 3-D network. [80]

*Table 4: Glass transition temperature ($T_g$), consolidation temperature $T_{CON}$ and total mass loss of melting gel synthesized by MTES-DMDES*

| MTES/ mol. % | DMDES/ mol% | $T_g$/°C before | $T_g$/°C after | $T_{CON}$/°C | Total Mass loss/ % |
|---|---|---|---|---|---|
| 50 | 50 | -56.7 | -- | 160 | 45 |
| 60 | 40 | -37.7 | -- | 155 | 47 |
| 65 | 35 | -18.8 | 3.1 | 150 | 35 |
| 70 | 30 | -6.4 | 9.4 | 145 | 34 |
| 75 | 25 | -0.3 | 17.3 | 135 | 30 |

## *Corrosion Protection*

Corrosion of metal surfaces is a natural process in air, which is 20% oxygen. The surface comes in contact with the surrounding environment and the metal is converted to a more chemically stable form such as oxides, hydroxides or sulfates. According to the World Corrosion Organization, the annual cost of corrosion worldwide is at $2.2 trillion, over 3% of the world's GDP.[81] Corrosion protection of metallic surfaces, as mentioned, is an increasingly expensive issue with an environmentally harmful solution, chromate paints. Despite its efficiency in protecting metals, hexavalent chromium can leach into

the environment, and the high oxidation properties of Cr(VI) cause problems in living organisms by damaging their DNA and causing cancer. ORMOSILs formed with traditional alkoxide precursors by sol-gel process have been used against corrosion for many years.[82] It is found that hybrid silicates provide good corrosion resistance, because they combine the mechanical and chemical characteristics of the organically modified silica networks. The corrosion protection films are durable, flexible and dense. The addition of organic components leads to thicker and more flexible films. Another advantage of the organic part of hybrid coatings is that it decreases the pore size and reduces cracking for barrier materials.

It is also found that sol-gel coatings have good adhesion both to metal and organic surfaces. Adhesion of sol-gel films to metals is possible by strong covalent Si-O-Me bonds that create corrosion stable metal-sol-gel interfaces. Considering that the adhesion of chromate treatments is based on mechanical interlocking, dispersion forces and hydrogen bonds in sol-gel films is a more stable solution.[83] Organic-inorganic hybrids can be tailored and modified to create materials that possess the desired properties like adhesion to organic paint systems. For example, silica based hybrid organic-inorganic coatings based on bisphenol A demonstrated efficient corrosion protection of aluminum alloy substrates against water and other corrosive agents. Zandi et al. found that sols with lower silane content had better corrosion resistance than sols with high silane content.[84]

The ease of applying ORMOSIL coatings is also an advantage, as there is a variety of types that can be used. Some of the techniques that have been used are spin coating, dip coating, inkjet printing, lithography, sputter deposition, electro- spraying.[85] In order to achieve good corrosion resistance, coating thickness, homogeneity, porosity,

hydrophobicity are some of the properties that must be tailored. Metroke showed that 3-glycidoxypropyltrimethoxysilane (GLYMO)–TEOS coatings exhibited high corrosion resistance for samples with high organic content and low hydrolysis content values. The benefit of these films is that a dense network is created providing a hydrophobic barrier that repels water and corrosion inhibitors.[86]

In the case of replacing chromate paints with hybrid sol-gel coatings, many types of coatings have been developed. Gels with 3-glycidoxypropyl-trimethoxysilane (GMPTS) as a precursor were doped with cerium nitrate. These composite coatings showed an improvement in the corrosion protection properties from the combination of the two materials.[87] MTES-DMDES melting gels were also investigated as corrosion protection coatings on stainless steel AISI 304 by Aparicio. The coatings were homogeneous and crack-free with good adhesion to the substrates and showed no variation between day one of immersion and after four months.[3]

# Experimental Techniques

## *Synthesis of melting gels*

The melting gels prepared for this project followed the synthesis process described previously by Klein and Jitianu for synthesis of melting gels using mono-substituted and di-substituted alkoxysiloxanes. The precursors used are methyltriethoxysilane (MTES) and dimethyldiethoxysilane (DMDES) (Sigma Aldrich, Milwaukee, WI) without any further purification or dilution. The molecular structures of the precursors are shown in Figure 10.

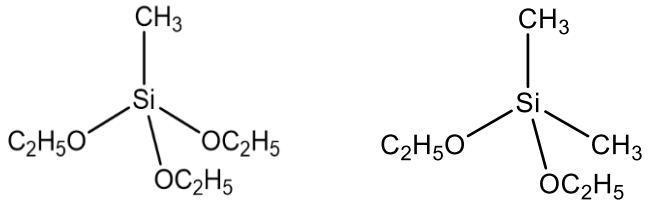


*Figure 10: Structures of precursors methyltriethoxysilane (MTES) and dimethyldiethoxysilane (DMDES) respectively*

The synthesis process including the introduction of gold nanospheres is shown in Figure 13. Hydrochloric acid and ammonium hydroxide were used as catalysts for the hydrolysis and polycondensation of the precursors as shown in the reactions in Figure 11. Anhydrous ethanol and deionized water were used during the synthesis. Finally, dry acetone was used for the removal of byproducts in the filtration step of the process.

$$CH_3Si(C_2H_5O)_3+H_2O \rightarrow (C_2H_5O)_2CH_3SiOH+C_2H_5OH$$

$$(CH_3)_2Si(C_2H_5O)_2+H_2O \rightarrow (C_2H_5O)CH_3SiOH+C_2H_5OH$$

*Figure 11: Hydrolysis reactions of MTES and DMDES*

The molar ratios used for the first step of the synthesis of MTES:EtOH:HCl:$NH_4OH$ were 1:4:3:0.01. For the addition of the di-substituted precursor the molar ratio was DMDES:EtOH 1:4. The melting gel precursor composition was 65% MTES-35% DMDES, 70% MTES-30% DMDES, and 75% MTES-25% DMDES.

Melting gel synthesis is complete in three stages. First, hydrochloric acid, DI water and half of the ethanol are mixed. Into that solution, the mixture of MTES with the other half of the ethanol is added dropwise, and the solution is stirred in a closed beaker for three hours at room temperature. The beaker is tightly covered with parafilm in order to prevent ethanol from evaporating.

After three hours of stirring, the second precursor is added to the solution. DMDES is mixed with ethanol in molar ratio 1:4 and added dropwise to the stirring solution. The container is sealed again with parafilm and the resulting solution is left stirring for two hours at room temperature.

The final step of the synthesis is to add ammonium hydroxide in the molar ratio mentioned above. After the addition of ammonium hydroxide, the solution is left stirring in a closed container for one hour and then the container is left open stirring for 48 hours at room temperature at low speed. The container is left open until gelation occurs.

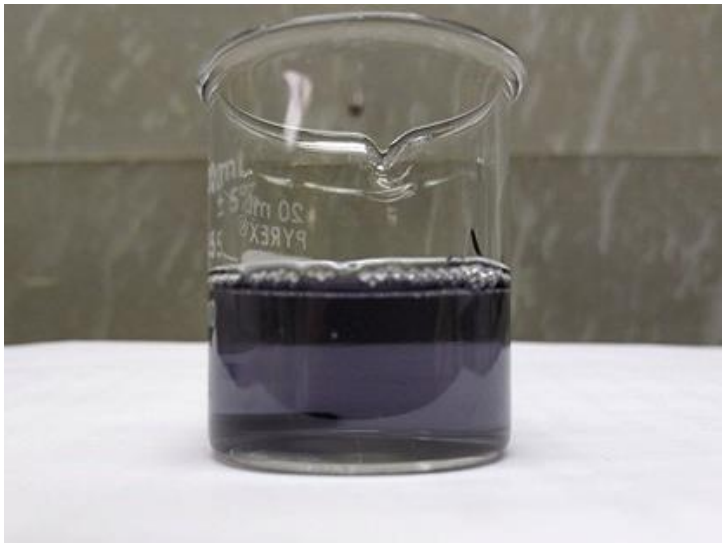

*Figure 12: Melting gel after the addition of Gold nanospheres*

In the last step of the synthesis process, a white powder is formed, which is ammonium chloride. In order to remove the ammonium chloride powder, 10 ml of dry acetone are added to the gelled product and stirred for an hour in a closed system. Subsequently, the solution was filtered by vacuum filtration for the removal of ammonium chloride.

The incorporation of nanoparticles in the melting gel is performed by the addition of resuspended gold nanospheres in dry acetone. The clear colorless solution is stirred in an open container on high speed while a 2 ml solution of gold nanospheres is added. Stirring is continuous until the solution becomes a gel again. Figure 12 shows the appearance of the gel once the gold nanospheres have been added. The gel takes on a light violet color. The darkness depends on the concentration of the addition.

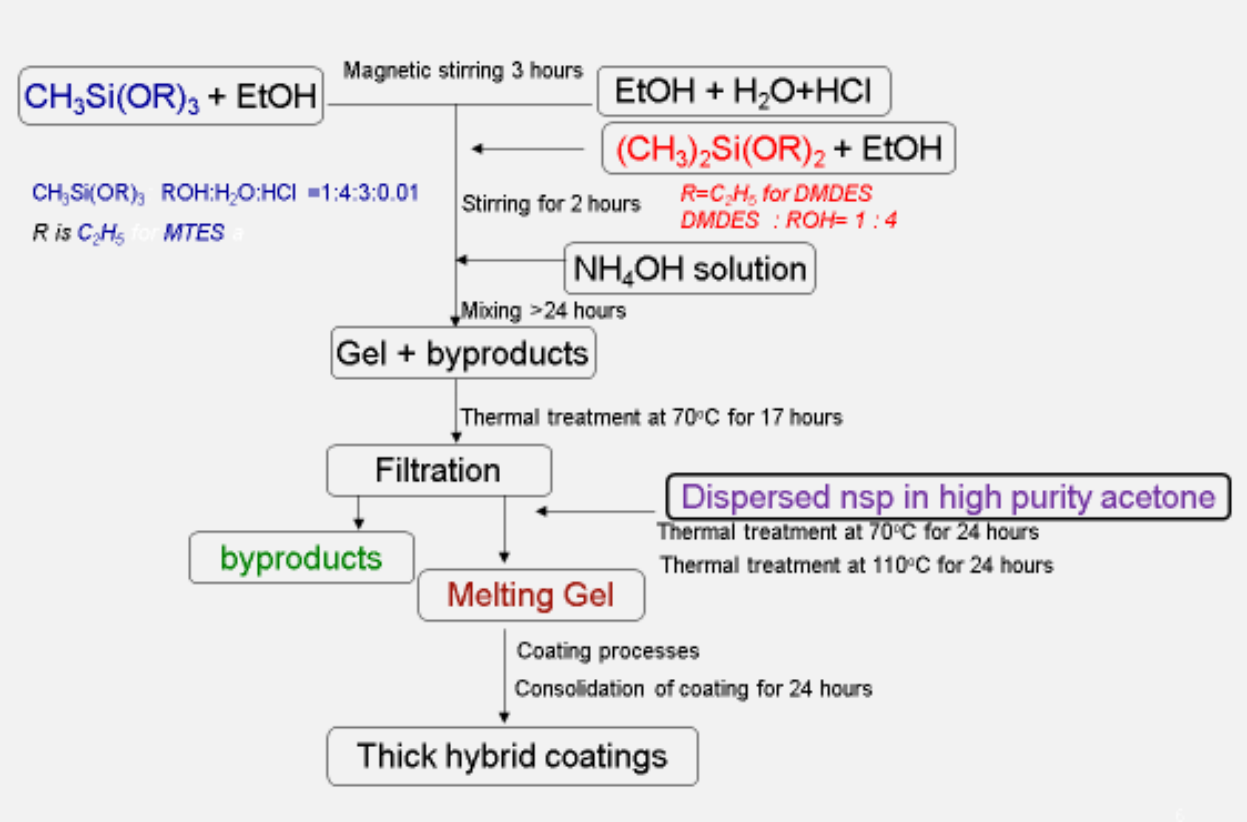


*Figure 13: Synthesis protocol chart of doped melting gel synthesis*

The process outlined in Figure 13 is followed by the last part of the modified hybrid gel thermal treatment. First the doped melting gel is heated at 70°C for 24 hours for the removal of the remaining organic solvents, ethanol and acetone. Next it is heated at 110°C for the removal of any remaining water.

The synthesis of doped melting gels is complete at this point. In some case, the next step is to make coatings of this material. Since melting gels are rigid at room temperature, it is necessary to make them more fluid in order to make coatings. The softening temperature where it is possible to pour the gel is typically about 110°C. For some coatings, a Corning™ glass slide is used as a substrate. The substrate is cleaned with aqua regia, DI water and isopropanol before the coating procedure. Then the substrate is heated at the same temperature as the melting gel for 15 minutes. Once the melting gel is fluid, a glass Pasteur pipette is used to transfer a small volume of melting gel onto the substrate. The gel flows onto the substrate to form a coating that is ~10 microns thick. The coated substrate is then heated at the consolidation temperature of the hybrid gel for 24 hours. Finally, the furnace that contains the samples is cooled down to room temperature slowly to avoid cracks of the coating. A sample of the consolidated hybrid silica glass is shown in Figure 14, on the left side is a coating of pure melting gel and on the right a doped melting gel with the addition of 10nM gold nanospheres.

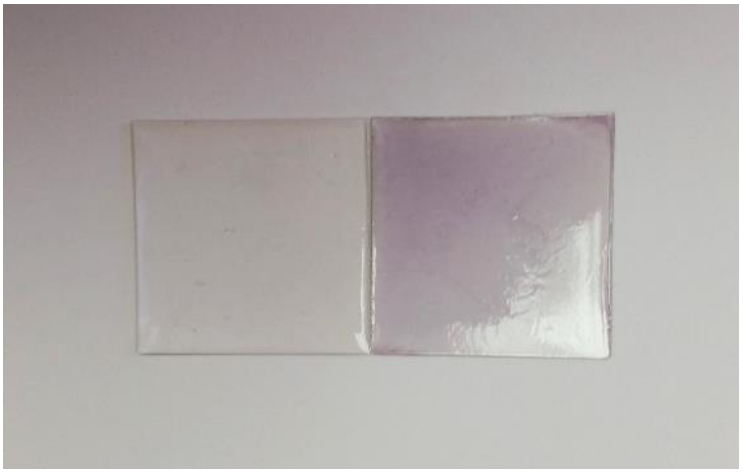

*Figure 14: Consolidated coatings of melting gels, pure on the left and with 10nM Gold nanospheres solution addition on the right.*

## *Synthesis of gold citrate nanospheres*

For the synthesis of the nanoparticles, a modified Turkevitch protocol was used. [63] In 186 ml of DI water 4 ml tetrachloroauric solution 0.025M was added. The solution was stirred while heating at 100°C until it started boiling. Then 10 ml of 1% trisodium citrate solution was added. Change of the color of the solution from light yellow to wine red was observed after 5 minutes of stirring. Then the solution was allowed to cool down while stirring at room temperature. Figure 15 shows the color of gold citrate nanospheres in water.

Sodium citrate is acting both as reducing agent and as a stabilizing agent for the nanoparticles. Centrifugation is required for the removal of excess solvent as well as the separation of light and heavy nanoparticles, to secure narrow size distribution. The nanoparticle solution was centrifuged at 7000 rpm for 50 minutes. Following the centrifugation, the supernatant was removed and the concentrated solution of Gold

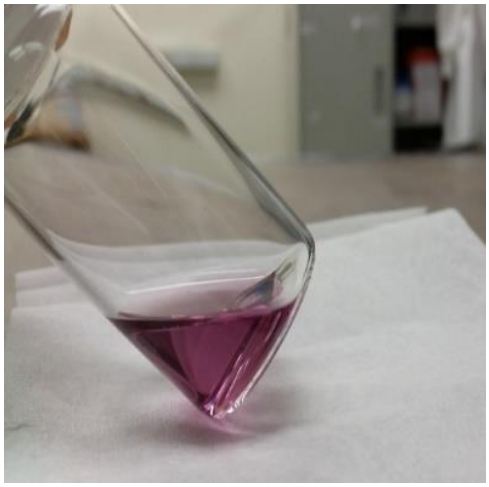

*Figure 15: Gold citrate nanospheres suspended in 2 ml acetone*

An hour before adding the gold nanospheres to the melting gel after filtration, a small amount of nanoparticles was added to 2ml of acetone. Table 5 shows the amount for each sample. Accordingly, the acetone suspended nanoparticles where added in the melting gel solution. When the gold nanospheres were added to the hybrid gel, a change of color was noticed from light red to purple.

*Table 5: Melting gels prepared for this project, precursor ratios and gold nanoparticle concentration of each sample.*

| **MTES-DMDES Molar Ratio** | **Au-nsps C (nM)** | **Au-nsps C (nM)** | **Au-nsps C (nM)** | **Au-nsps C (nM)** | **Au-nsps C (nM)** | **Au-nsps C (nM)** |
|---|---|---|---|---|---|---|
| 65%-35% | 0 | 8 | 10 | 12 | 14 | 18 |
| 70%-30% | 0 | 8 | 10 | 12 | 14 | 18 |
| 75%-25% | 0 | 8 | 10 | 12 | 14 | 18 |

## *Characterization Techniques*

The characterization techniques that follow have been divided depending on the state of the melting gel when the analysis performed was started. Listed first are the techniques used on fresh, not consolidated samples. The analyses used on hybrid glass were performed on samples that were poured on Corning glass substrates as thick films and then were heated isothermally at the consolidation temperature of each precursor ratio for 24hr and then cooled down slowly for 5 hours.

## *Melting gels*

### *Thermal analysis*

The thermal analysis of melting gels before their consolidation was studied using Thermogravimetric/Differential Thermal Analyzer (TG-DTA) (SII Nano Technologies Inc., Model TG/DTA6200 115V) and differential scanning calorimetry (DSC TA-Q-20). DSC analysis was performed in all three ratios of precursors for nanoparticle concentrations 0, 8, 10, 12, 14, 18 nM. The DSC analyses were recorded using a 5°C/min heating rate between -90 and 500°C in nitrogen flow (50 mL/min). Thermogravimetric analysis was performed on doped and undoped melting gel samples with ratios 65% MTES – 35% DMDES, 70% MTES – 30% DMDES, 75% MTES -25% DMDES. DTA and TG were recorded at 5 °C/min heating rate in the temperature range between 50 and 800°C under air flow (100 mL/min).

DSC is used to identify the glass transition temperature $T_g$, which is the interval between the glassy state and the liquid state of a polymer. It should increase with an increase in the number of oxygen bridges between silicon atoms. Decrease of the $T_g$ for

the gold-doped samples might indicate a decrease in the number of the oxygen bridges or a change in the relaxation times of polymer segments.

## *Oscillatory Rheometry*

The viscosity at low temperatures and the rheological properties were investigated using oscillatory rheometry (TA AR-G2, using a 3°C/min heating rate in air) on melting gels before their consolidation. The temperature sweep oscillatory measurements were performed from room temperature to -100°C, with a temperature ramp of -3°C/min at a constant stress of 100Pa. The oscillatory frequency was chosen according to the linear viscoelastic domain for each gel. This was determined by performing frequency sweep tests prior to the temperature sweep tests. For samples 75%MTES - 25%DMDES and 70%MTES - 30%DMDES, frequency $\omega_0$ has been set at 6.283 rad/s, while for the remaining three samples, $\omega_0$ has been set at 0.6283 rad/s. When the glass transition temperature was reached for each gel, the temperature sweep test was stopped.

The complex viscosity ($\eta$) was estimated from the values of viscous modulus, G'' and the angular frequency, $\omega_0$ ($\eta$=G''/$\omega_0$). The temperature dependence for the viscosity was evaluated assuming that viscosity is an activated process, according to an Arrhenius model ($\ln\eta=A+E_a/RT$, where A is a preexponential factor, $E_a$ is the activation energy to reach the vitreous state, and R is the ideal gas constant, 8.3145 J/mol K).

### *FT-IR*

Fourier transform infrared spectroscopy was performed for two samples of each precursor ratio without gold nanospheres and with 14nM gold nanospheres. The experiment was held for fresh melting gels in a heating ramp until their consolidation temperature with NICOLET IS50 FT-IR. The experiment started at 25° where the sample was held for five minutes. Then the sample was heated at a constant rate 5°C/min, the same rate as DSC. FT-IR spectra were collected every two minutes after the first minute of heating until the sample reached the consolidation temperature.

The Table below has the consolidation temperatures for each ratio of precursors that was studied. After the sample reached the consolidation temperature, it was held at the same temperature for 90 minutes and a spectrum was recorded every 10 minutes.

## *Hybrid Glass*

### *UV-Visible Spectroscopy*

Because of the addition of an optical material in the hybrid silica network UV-Vis spectroscopy was used to measure the absorbance of hybrid silica glasses undoped and doped. An initial test of the nanoparticle stability was performed by measuring the UV-Vis spectra of gold nanospheres dispersed in acetone for 24 hours. For these two measurements spectra were acquired by SI Photonics Model 440 Spectrometer (Tucson, AZ). During the preparation of gold nanospheres, the absorbance was measured by Thermo Scientific Nanodrop 2000 (Waltham. MA).

## *TEM*

Transmission Electron Microscopy was used to image the gold nanoparticles in the hybrid glass. Conventional imaging techniques had failed to show how the nanoparticles were dispersed in the melting gel. The samples for TEM were consolidated and then broken into smaller pieces these pieces were encapsulated in Spurr low viscosity resin. Then the encapsulated samples were cut in thin slices with a Leica Reichert Ultraacut S microtome. The TEM used was JEOL 1200EX electron microscope with AMT-XR41 digital camera with 80KV power. The surface and cross-section of doped hybrid silica glasses of each precursor ratio was imaged.

## *Small Angle X-Ray Scattering (SAXS)*

Hybrid Silica gels were studied with SAXS to investigate the microstructures of the doped glass like independent nanoparticles or agglomerations. SAXS scattering experiments were conducted at the ultra-small angle X-ray scattering (USAXS) instrument at the Advanced Photon Source, Argonne National Laboratory. A Bonse-Hart type of crystal optics is used by this machine to access a scattering $q$ range that is normally unavailable to a conventional pinhole based small angle scattering camera. Here $q$ is the magnitude of the scattering vector, and is defined as $q = 4\pi/\lambda \sin(\theta)$, where $\lambda$ is the X-ray wavelength and $\theta$ is one half of the scattering angle. The USAXS instrument has a $q$ resolution of $\approx 1 \times 10^{-4}$ Å$^{-1}$. Coupled with an add-on Pilatus 100K detector, the USAXS instrument can access a $q$ range from $1 \times 10^{-4}$ Å$^{-1}$ to 1 Å$^{-1}$.

1D-collimated USAXS experiments were conducted in fly-scan mode using monochromatic 17.5 keV X-rays ($\lambda$ = 0.708481Å). The beam size was 0.8 mm × 0.8 mm.

The X-ray flux density was ≈ $10^{13}$ photon $s^{-1}mm^{-2}$. The high X-ray flux ensures that weak scattering signals, commonly expected from a melting gel system, be captured. Total scan time was 120 s. The sample was placed on a standard sample holder.

## *Raman spectroscopy*

Raman spectroscopy was performed using a Renishaw inVia-Reflex Micro-Raman 532nm Laser at 10% power for consolidated melting gel samples on a Corning™ glass substrate. The extended spectra were recorded from 0-3300 wavenumbers ($cm^{-1}$) with 10 s exposure. Raman spectra of consolidated melting gels of all three ratios were recorded for samples without nanoparticles and with nanoparticle concentration of 10 nM.

# Results

## *Nanoparticles Characterization*

The synthesis of hybrid silica gels modified by gold citrate nanospheres started with the synthesis of the nanoparticles. Gold citrate nanospheres were synthesized according to the protocol stated in the experimental section. The shape and size were investigated with TEM. Micrographs of the nanoparticles, as captured on grids, are shown in Figure 17. According to these micrographs, the nanospheres have diameters around 16nm and are uniform in shape. Dynamic Light Scattering (DLS) also confirmed the diameter to be 16nm with a very narrow size distribution.

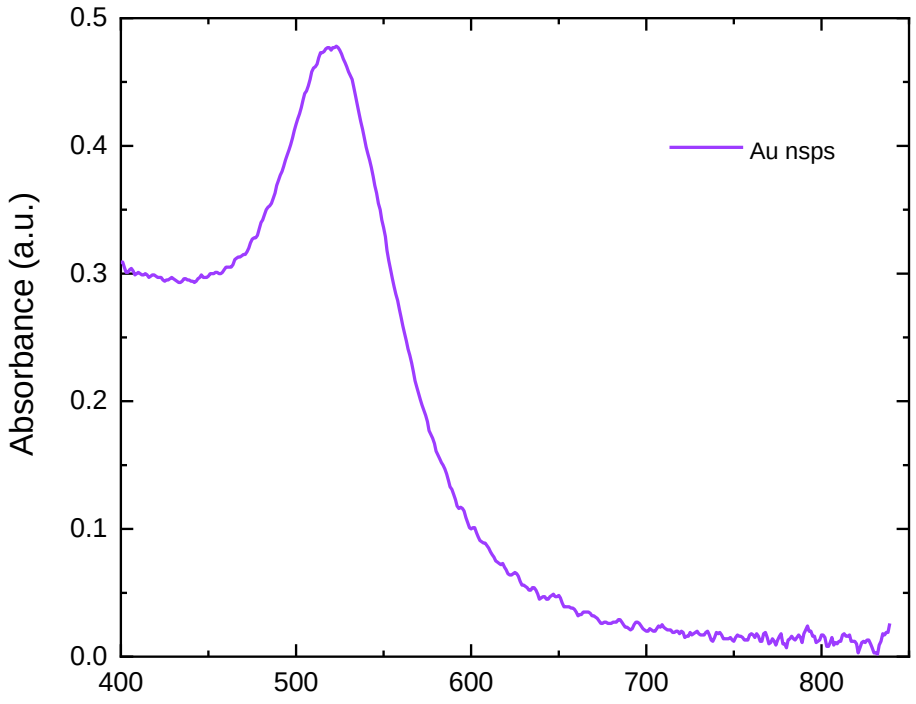


*Figure 16: UV-Vis spectra of gold citrate nanospheres in water.*

The UV-Vis spectra of the nanoparticles were obtained in water and the plasmon position was recorded at ~520 nm as shown in Figure 16. A check of their stability was critical to the goal of this project. The evaluation of the nanoparticle stability was carried out before incorporating them into the melting gels. Monitoring of the gold nanospheres following centrifugation and resuspension in acetone was carried out by collecting UV-Vis spectra. As known from the literature, each nanoparticle morphology has a corresponding plasmon peak, which is the result of the collective oscillation of the free electrons. By observing the shape and position of the plasmon peak of gold nanospheres, the stability of the suspension was determined.

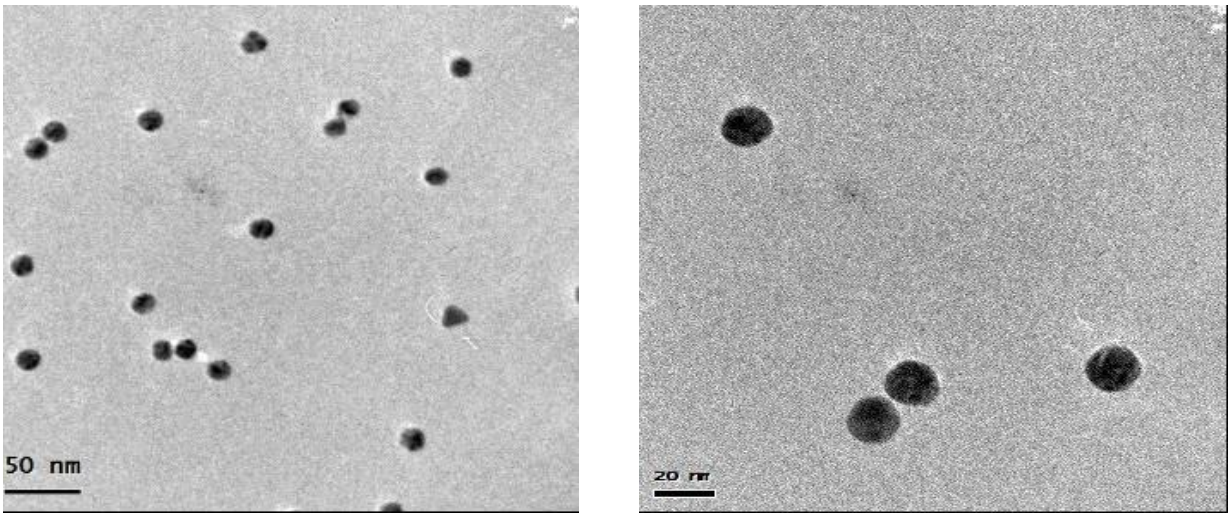


*Figure 17: Micrograph collected with TEM showing 16nm gold nanospheres.*

The solution used for this analysis was kept in a quartz cuvette, sealed, in order to minimize acetone evaporation. The spectra of the nanoparticle suspension are shown in Figure 19. In (a) the spectra of the first 8 hours is presented, in (b) from hour 8 to hour 15 and in (c) 16 to 24 hours. The position of the plasmon peak did not change throughout the 24 hours.

Since the stability of gold nanospheres after incorporation into melting gels was unknown, it was critical to determine their stability before incorporation. This eliminated changes before incorporation as a variable in the study. Having confirmed that the nanoparticles are stable after the change of solvent from water to acetone, gold nanospheres were introduced into sol-gel mixtures. In Figure 18, a series of hybrid gels doped with various concentrations of gold nanospheres is shown.

For all three precursor ratios, the sol-gel process was followed as described before. The new aspect was the addition of gold nanospheres dispersed in acetone after the filtration process. The nanoparticles were stored in water at 4°C prior to the solvent transfer which was performed 10 minutes before the addition to the sol-gel mixture. The process continued as described in the experimental section and doped melting gels of different precursor ratios were doped with five different concentrations. All doped samples developed a violet color indicating the nanoparticle presence as shown in Figure 19. By increasing the concentration of nanoparticles, the intensity of the color was increased.

*Figure 18: 65%MTES- 35%DMDES melting gels with Au-nsps concentrations from left to right 8,10,12,14,18nM*

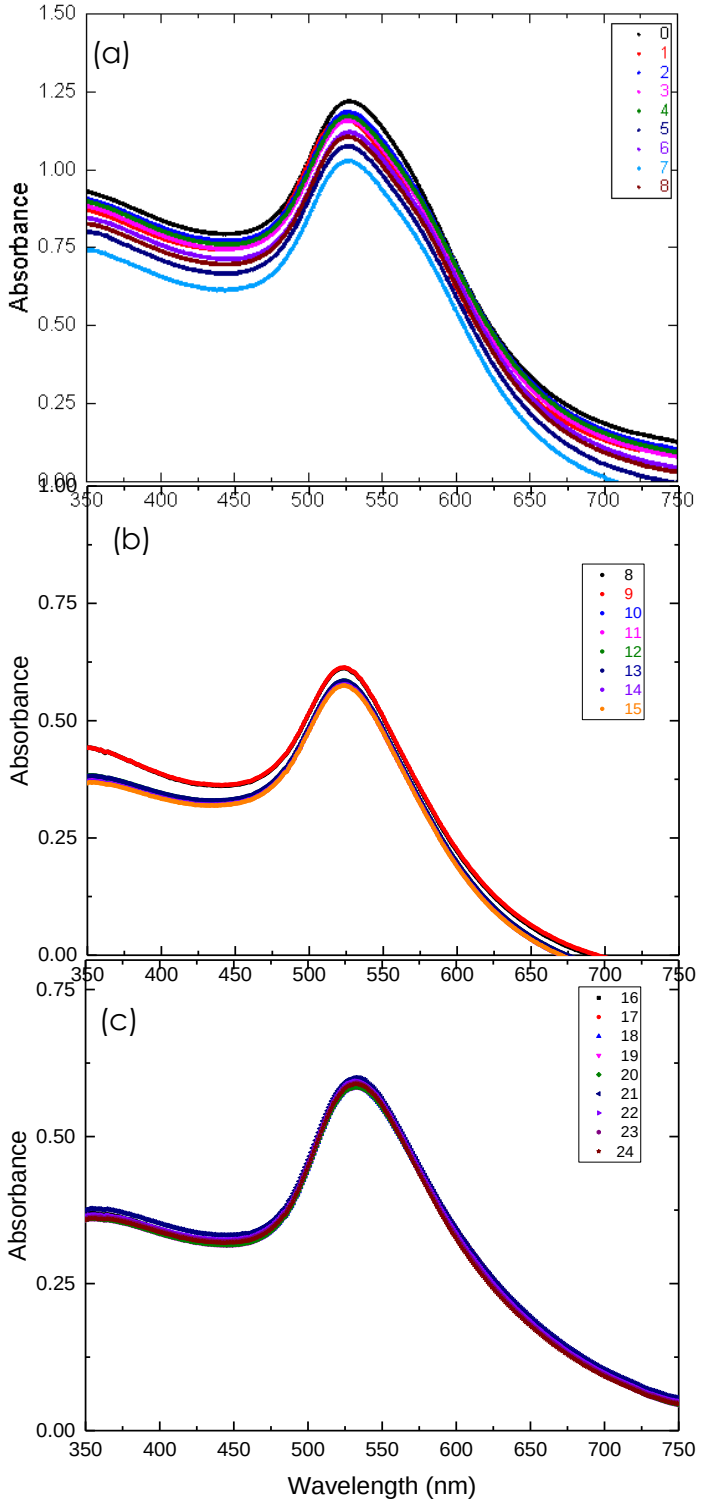


*Figure 19: UV-Vis spectra of citrate gold nanospheres resuspended in acetone for 24 hours: (a) 0-8 hours, (b)8-15 hours, (c) 9-14 hours.*

## *Melting Gel Characterization*

During the transfer of the doped melting gels in order to prepare coatings, a difference in viscosity was noticeable. The change in viscosity was investigated in detail using oscillatory rheometry. The frequency chosen for each sample was determined by sweep tests.

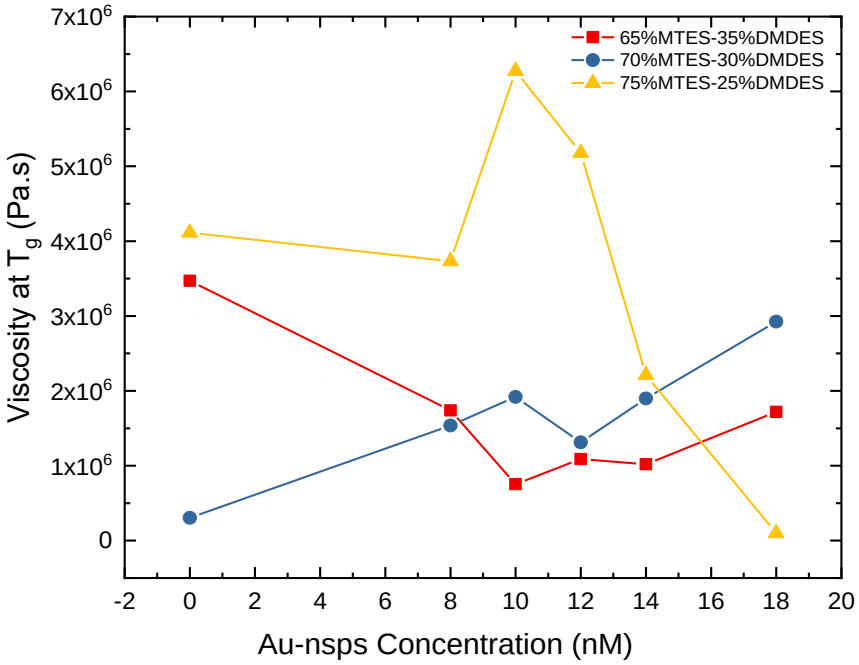


*Figure 20: Viscosity of melting with respect to the nanoparticle concentration at the glass transition temperature of each melting gel.*

Each melting gels was subjected to shear stress. The temperature was decreased from room temperature until the glass transition temperature for each gel was reached. Using the values of G" the viscous modulus and the angular frequency of test $\omega_0$, the complex viscosity at the glass transition temperature was determined ($\eta=G''/\omega_o$) as shown in Figure 20. [88]

Each composition of melting gel responded differently to the addition of nanoparticles. For 65%MTES-35%DMDES, the viscosity went through a minimum and then increased again. In the case of 70%MTES-30%DMDES, there was a continuous increase in

the viscosity with an increase of the nanoparticle concentration. In the case of 75%MTES-25%DMDES, the viscosity went through a maximum at 12nM, the same concentration as the minimum of 65%MTES-35%DMDES.

The oscillatory rheometry measurements allow also the direct determination of the glass transition temperature $T_g$. The two components of complex modulus $G^*$, elastic modulus G' and viscous modulus G'' were measured in a small amplitude oscillatory shear as a function of decreasing temperature. The angular frequency was held constant during the temperature sweep tests. $T_g$ was assigned at the temperature where the two lines of the moduli intersect.

In Figure 21 , the elastic and viscous moduli versus temperature are shown for the 65%MTES-35%DMDES composition. The $T_g$ obtained by oscillatory rheometry is also shown in Figure 21, and the same trend is followed by two of the three compositions. Both 65%MTES-35%DMDES and 75%MTES-25%DMDES show a decrease in the glass transition

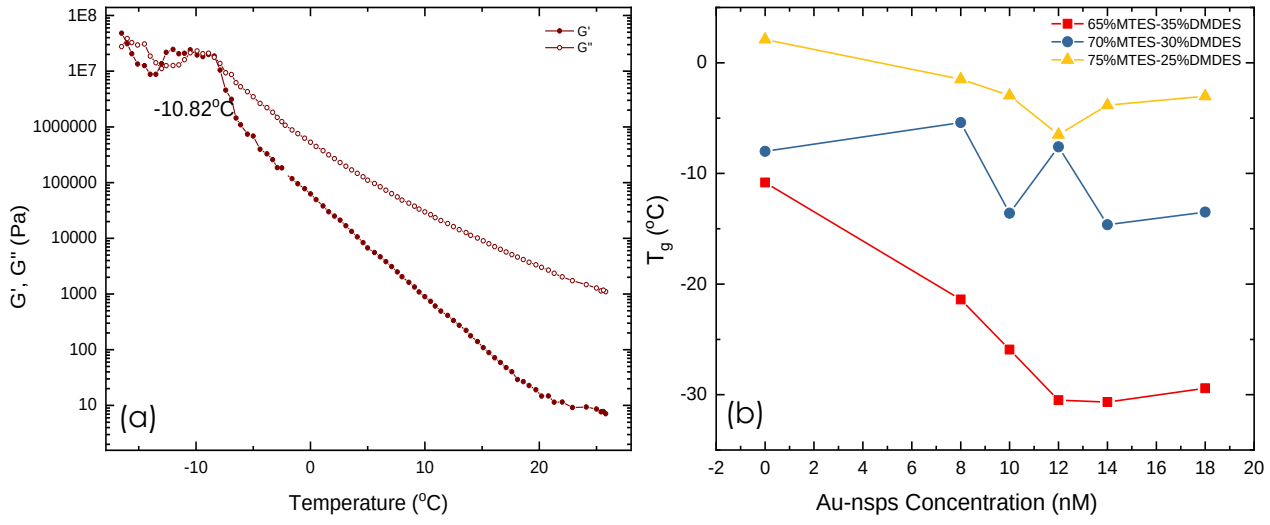


*Figure 21: (a) Elastic (G') and viscous modulus vs temperature for melting gel 65%MTES-35%DMDES (b )glass transition temperature obtained by oscillatory rheometry with increasing nanoparticle concentration*

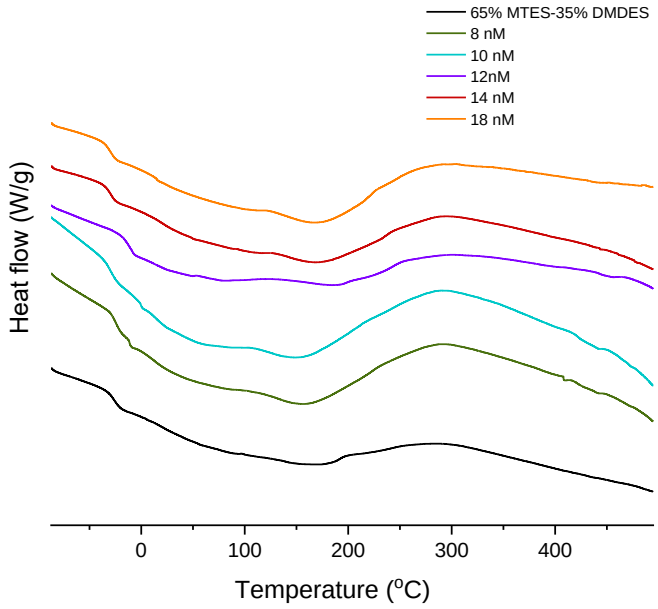


*Figure 22: DSC curves for melting gels heated with nitrogen at rate 5°C/ min 65%MTES-35%DMDES MG from 0 to 18nM Au-nsps, top to bottom*

temperatures until 12nM, where they both have a minimum. At the two higher concentrations, both show an increase. Further thermal analysis on the doped and undoped melting gels was performed. The glass transition temperatures of all of the samples were recorded with Differential Scanning Calorimetry (DSC). Samples of all compositions at melting gel form were heated at 5°C/ min rate in nitrogen atmosphere.

The DSC curves are shown in Figures 22 and 23 present an exothermal peak around 260°C, when nanoparticles are introduced into the system. The resulting curves show a wider exothermal peak for 65%MTES-35%DMDES a nd 75%MTES-25%DMDES. All of the curves presented in Figures 22 and 23 present the same general trend with slight differences. A comparison between the $T_g$ obtained with oscillatory rheometry and the $T_g$ from DSC is reported at Table 9.

A comparison between the glass transition temperatures obtained with Thermogravimetric Analysis combined with Differential Thermal Analysis were performed on melting gels. The analyses were performed on two samples for each ratio of precursors, one sample had gold nanoparticles at 10nM, whereas the other was undoped.

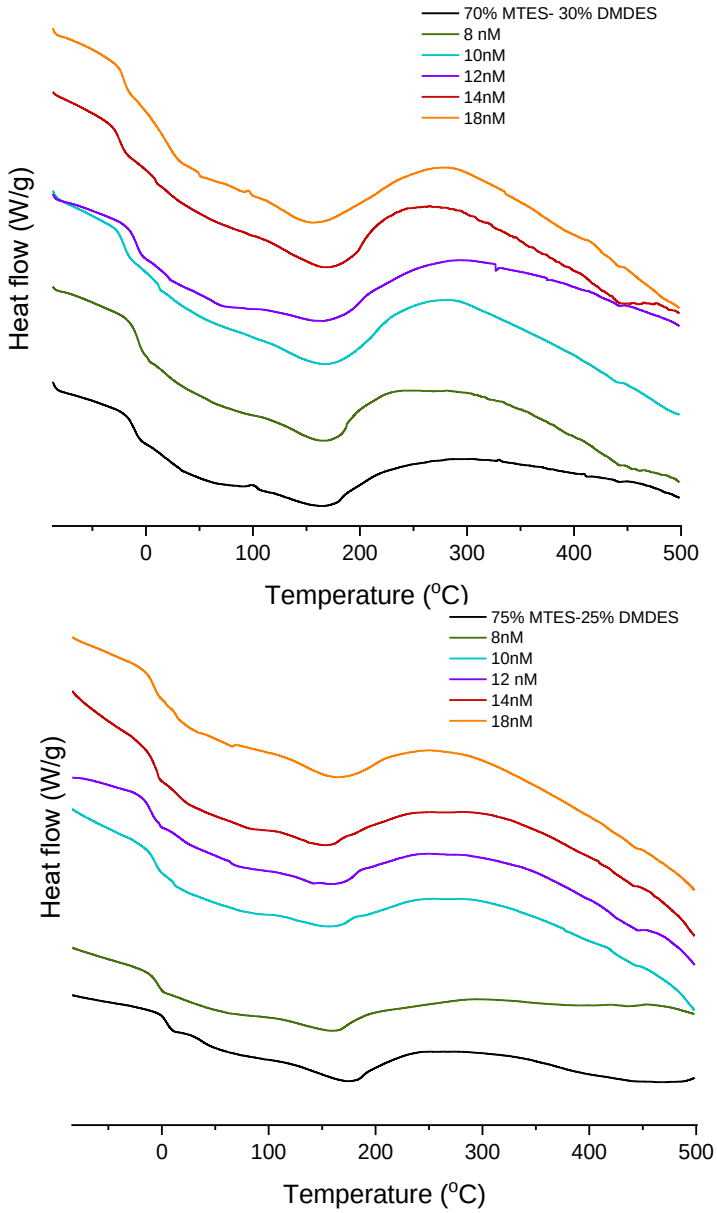


*Figure 23: DSC curves for melting gels heated with nitrogen at rate 5°C/ min 70%MTES-30%DMDES and 75%MTES-25%DMDES MG from 0 to 18nM Au-nsps, top to bottom*

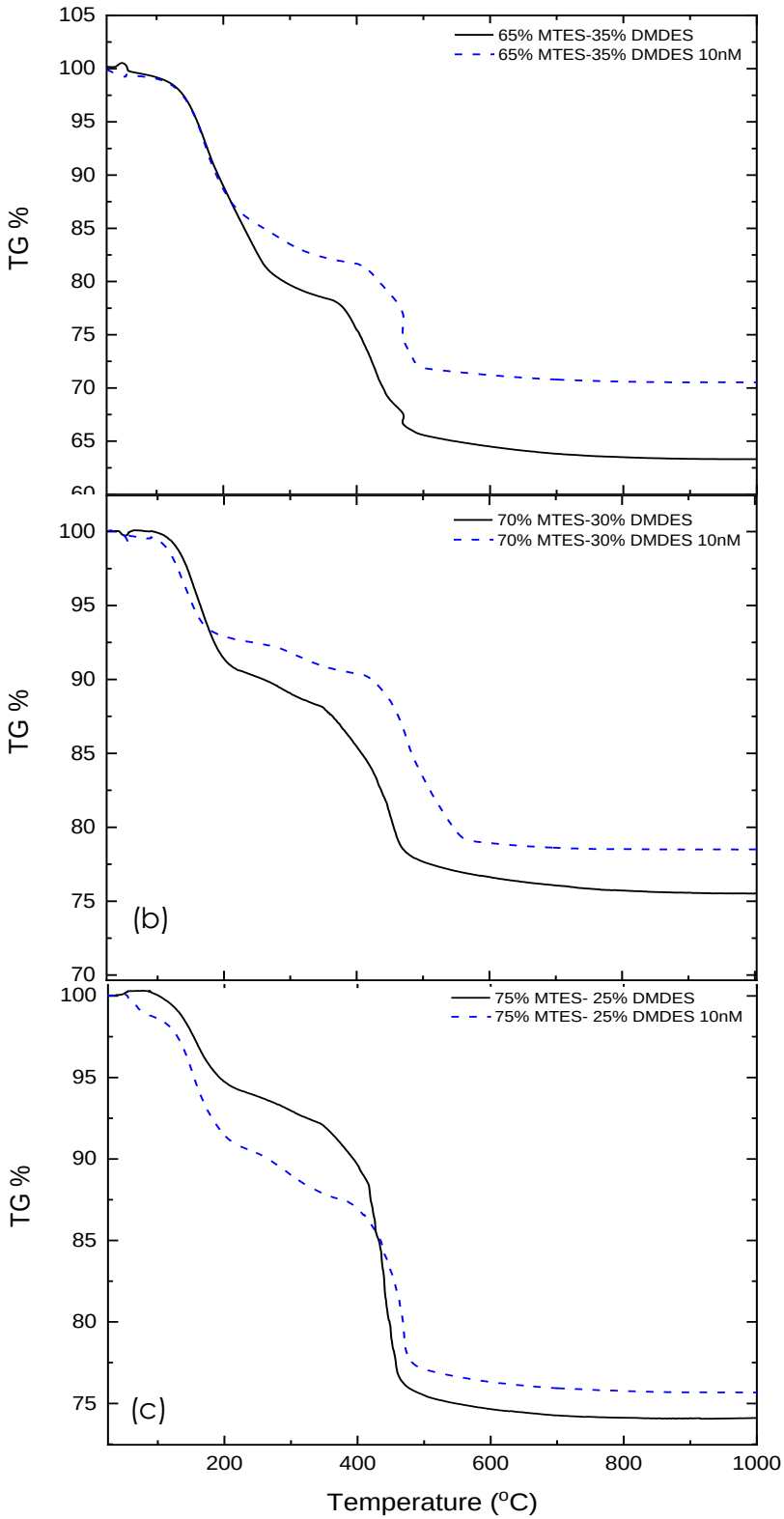


*Figure 24: TG% data of doped and non-doped melting gels (a) 65%MTES-35%DMDES, (b) 70%MTES-30%DMDES, (c) 75%MTES-25%DMDES*

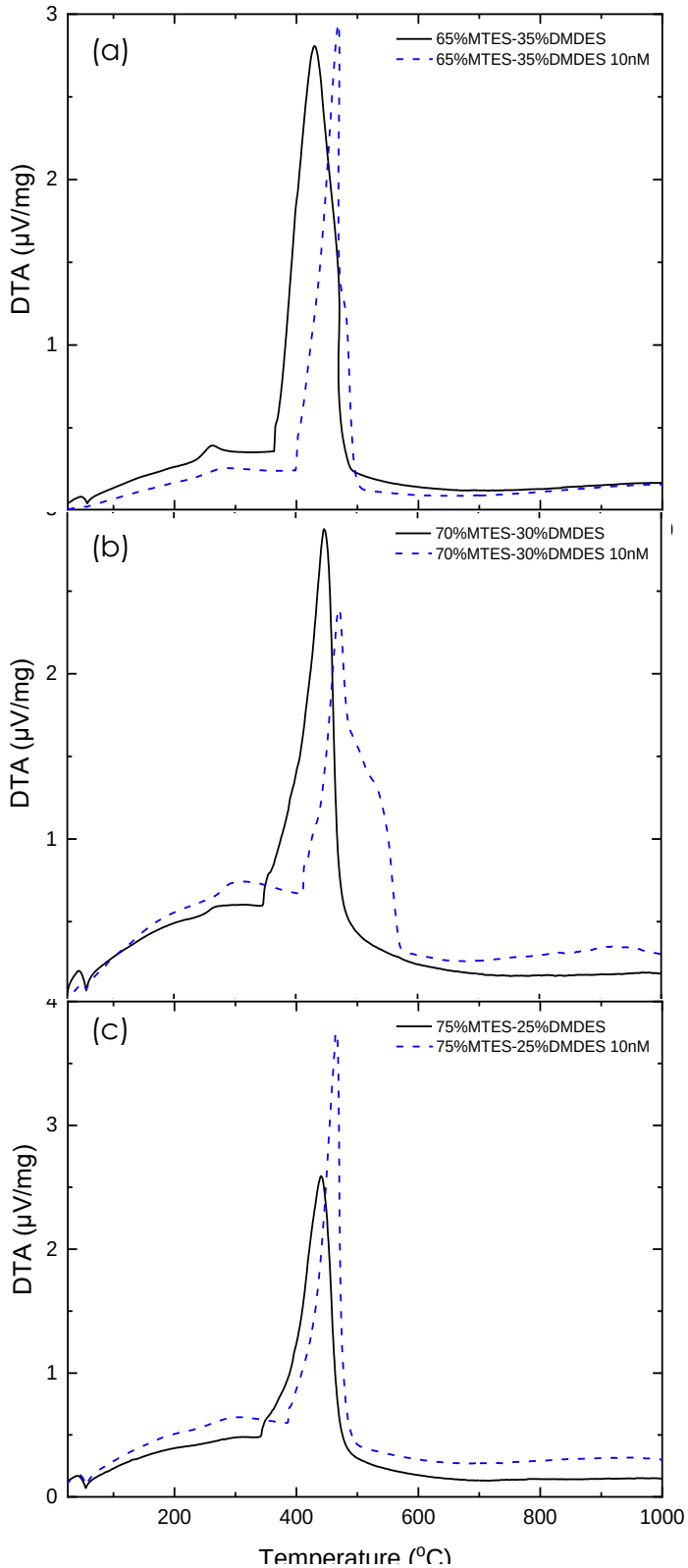


*Figure 25: DTA% data of doped and non-doped melting gels (a) 65%MTES-35%DMDES, (b) 70%MTES-30%DMDES, (c) 75%MTES-25%DMDES (MG solid line, MG with 10nM Au-nsps dashed line)*

Figure 24 shows the TG curves of all the samples paired according to the precursor ratio. The % mass loss is divided in two steps, the first one is from 150 to 280°C and the second step occurs between 360 and 490°C. The first step corresponds to the removal of residual unreacted alkoxide precursors and is correlated with the small exotherm around 270°C attributed to oxidation of residual ethoxy groups. The second step is correlated with the high exothermal peak around 440°C which is assigned to the combustion of methyl groups. For all of the samples, the mass loss is lower in total for the samples containing gold nanospheres. The % mass loss is reported in Table 6, with the percentages based on the step of the thermal decomposition of the sample.

*Table 6: %Mass Loss for each step of the process and total Mass Loss of each sample, obtained by TGA*

| **Step** | **65%-35%** | **65%-35% 10nM** | **70% -30%** | **70%-30% 10nM** | **75%-25%** | **75%-25% 10nM** |
|---|---|---|---|---|---|---|
| 1st Step | 30.7 | 20.5 | 19.3 | 10.78 | 21.1 | 15.9 |
| 2nd Step | 5.4 | 8.1 | 6.7 | 10.08 | 5.1 | 7.4 |
| Total %Mass Loss | 36.1 | 28.6 | 26.0 | 20.86 | 26.2 | 23.3 |

The first step results in higher mass loss percentage compared to the second one. The largest difference is seen for 65%MTES-35%DMDES melting gel with a difference of 25.3% between the two steps. The lowest difference between the two steps is reported for 70%MTES-30%DMDES with 10 nM concentration of nanoparticles at 0.7%.

The DTA curves are shown in Figure 25 the doped melting gels with a dashed line and the melting gels without nanoparticles with a solid line. In Fig. 25 the DTA curves for

all three ratios show two peaks that correspond to the mass loss of the hybrid silica network as described above in the TGA curve description. The shift between the curves from lower temperatures for non-doped samples to higher temperatures for doped samples is evident.

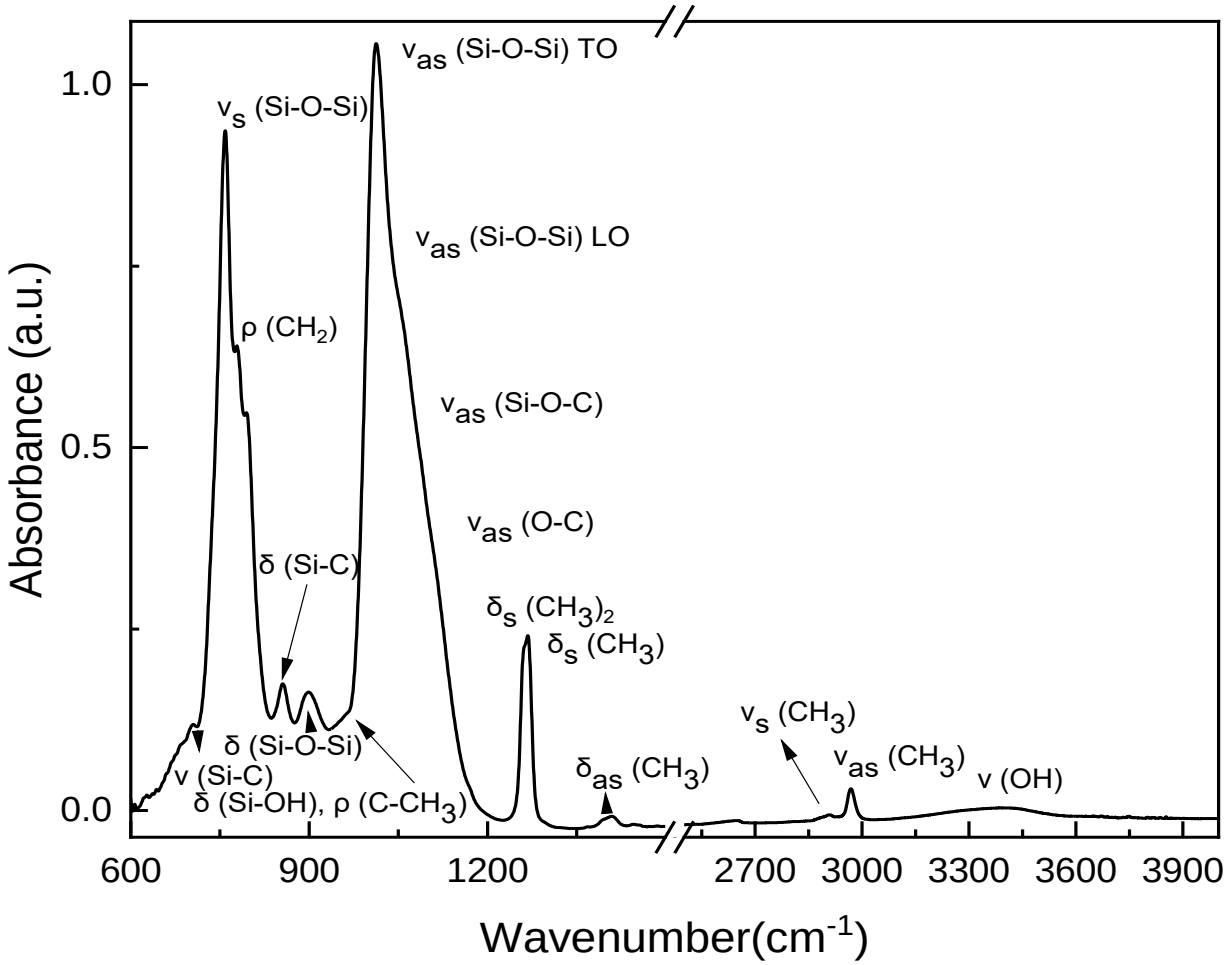


*Figure 26: FT-IR spectrum of 65%MTES-35%DMDES melting gel at 25°C*

The last analysis performed on unconsolidated melting gels was FT-IR. As in TG-DTA, all precursor compositions were analyzed on pairs of samples, one with nanoparticle concentration of 14nM and one without nanoparticles. A protocol was developed in order to study the evolution of the consolidation process with FT-IR. Starting at 25°C, the sample was heated at 5 °C/min rate until the consolidation temperature of each

composition and then it was held isothermally at the consolidation temperature for 90 minutes. Spectra were collected while the sample was heating at a steady rate, and while the sample was held isothermally at the consolidation temperature. For the 65%MTES-35%DMDES composition, spectra were also collected in the hybrid glass form.

A representative spectrum of 65%MTES-35%DMDES is shown in Figure 26 for 25°C. All of peaks are shown with the assignments according to literature. In Figure 26 above, the inorganic and organic components of the network are identified. The highest intensity peaks are associated with the Si-O-Si part of the network, whereas the organic components give rise to lower intensity peaks.

A complete list of peak assignments is reported in Table 7, where each vibrational mode is listed for four different states of the 65%MTES-35%DMDES melting gel. First, the assignments are for the sample at 25 °C while it is still a gel. The second column is at the melting temperature which is 110°C. The third column is at the consolidation temperature at 150 °C, and the last one is for a consolidated sample at 25°C.

In the Table, it is seen that there are some shifts in the position of the peaks. The most evident peak with changes is ν (Si-OH), ρ (C-$CH_3$), which at 25 °C is located at 953 $cm^{-1}$ for the unconsolidated sample, while in its hybrid glass form, the peak is located at 962 $cm^{-1}$. Another peak that has a shift is $\nu_{as}$ (Si-O-Si) TO. The peak has a position at 1012 $cm^{-1}$ for 65%MTES-35%DMDES melting gel at 25 °C, while it shifts to 1006 $cm^{-1}$ for consolidated sample. The area that is assigned to ν (OH) is also shifting according to temperature, and not state of the melting gel. For lower temperatures, the peak is in the area 3150-3450 $cm^{-1}$ and for higher temperature the area is shifting to higher wavenumbers.

*Table 7: Peak assignments of FT-IR spectra collected from 65% MTES- 35% DMDES MG at 25°C, 110 °C, 150 °C and from hybrid glass at 25 °C.*

| Peak assignment | Wavenumber ($cm^{-1}$) 25°C MG | Wavenumber ($cm^{-1}$) 110°C MG | Wavenumber ($cm^{-1}$) 150°C MG | Wavenumber ($cm^{-1}$) 25°C HG |
|---|---|---|---|---|
| ν (Si-C) | 704 | 703 | 703 | 704 |
| $\nu_s$ (Si-O-Si) | 758 | 758 | 758 | 758 |
| ρ ($CH_3$) | 778 | 778 | 778 | 777 |
| δ (Si-O-C) | 856 | 854 | 853 | 855 |
| δ (Si-C) | 898 | 917 | 917 | 898 |
| ν (Si-OH), ρ (C-$CH_3$) | 953 | 953 | 955 | 962 |
| $\nu_{as}$(Si-O-Si)TO | 1012 | 1010 | 1011 | 1006 |
| $\nu_{as}$(Si-O-Si)LO | 1056 | 1061 | 1062 | 1067 |
| $V_{as}$(Si-O-C) | 1091 | 1088 | 1086 | 1089 |
| $V_{as}$(O-C) | 1117 | 1112 | 1114 | 1115 |
| $\delta_s(CH_3)_2$ | 1262 | 1262 | 1262 | 1262 |
| $\delta_s$ ($CH_3$) | 1268 | 1268 | 1268 | 1268 |
| $\delta_{as}$ ($CH_3$) | 1408 | 1406 | 1406 | 1409 |
| $\nu_s$ ($CH_3$) | 2908 | 2909 | 2910 | 2909 |
| $\nu_{as}$ ($CH_3$) | 2968 | 2968 | 2968 | 2969 |
| ν (OH) | 3149-3554 | 3329-3723 | 3329-3723 | 3145-3463 |

## *Hybrid Glass Characterization*

When a melting gel is held at its characteristic consolidation temperature, it crosslinks forming a hybrid organic-inorganic glass. The first analysis that was used to study the doped melting gels was UV-Visible spectroscopy. The melting gels were deposited on a glass substrate and heated up at the consolidation temperature for 24 hours. The resulting glass coatings were used to investigate the absorbance of the new material.

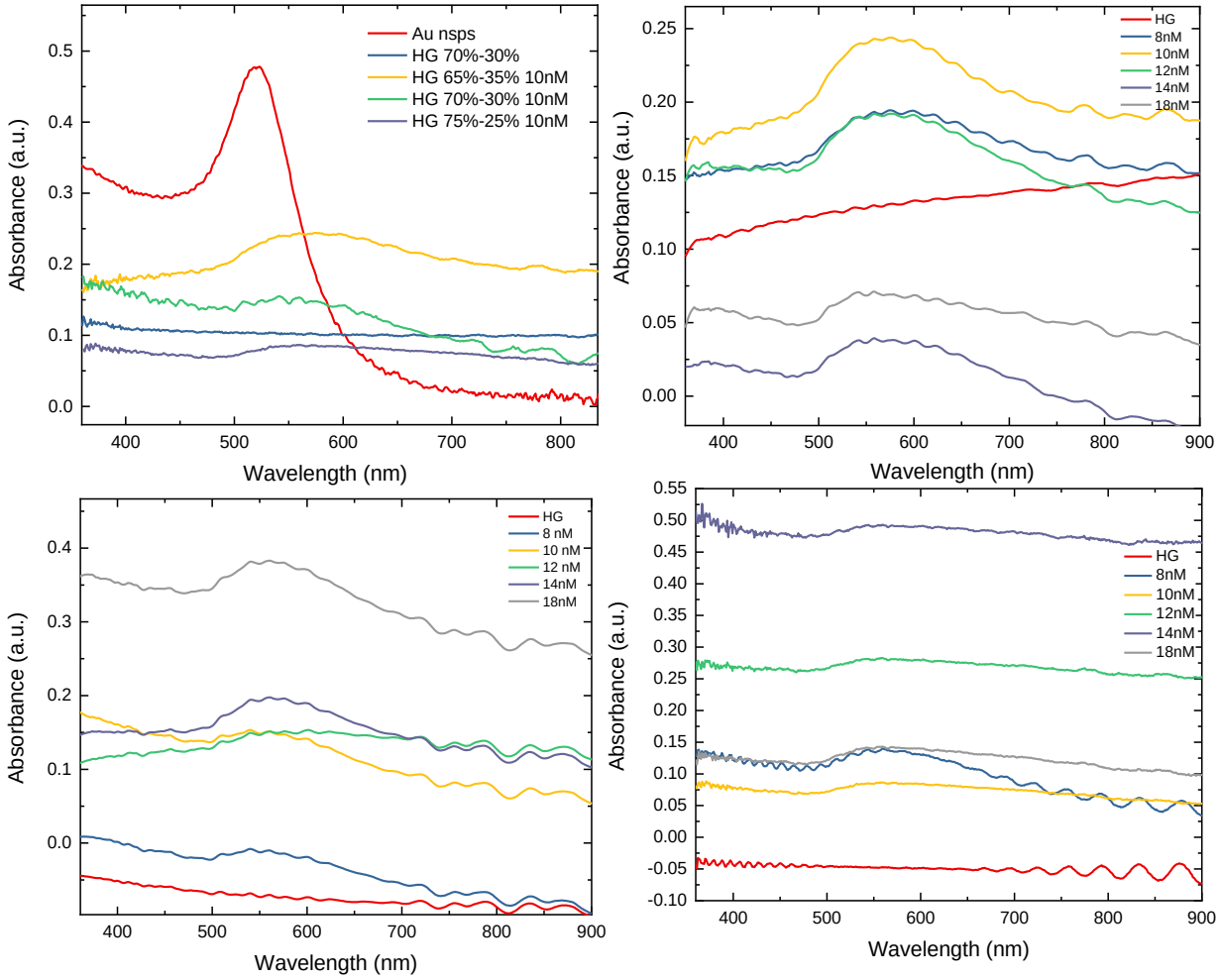


*Figure 27: UV-Vis spectra (a) comparison of Au-nsps dispersed in water, hybrid glass, doped hybrid glasses (b) hybrid glass of 65%MTES-35%DMDES with increasing concentrations of Au-nsps, (c) hybrid glass 70%MTES-30%DMDES with increasing concentrations of Au-nsp*

In Figure 27, the UV-Vis spectra are shown for all three compositions, with all of the nanoparticle concentrations. All of the doped samples present a wide absorption band around 560 nm, while the undoped samples have linear spectra. The absorption band is the result of the nanoparticle doping, contributing their plasmonic properties to these composites.

The plasmon of the nanoparticle suspension at 519 nm has widened and shifted, when the nanoparticles are incorporated into the melting gel. Differences observed in the shape and intensity of the plasmon peak are related to the new medium that hosts

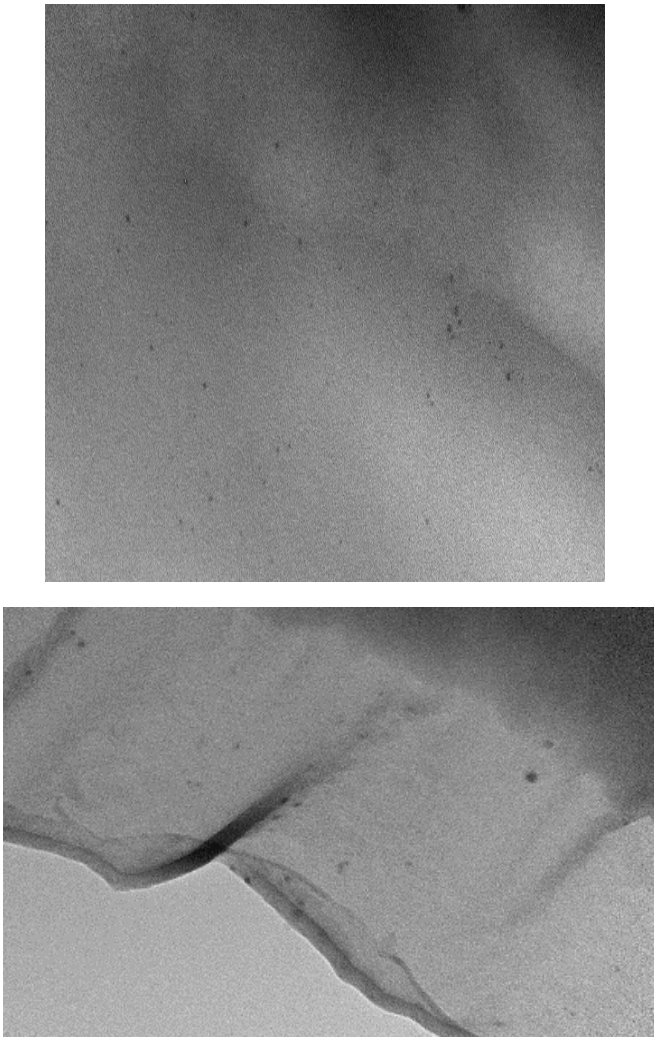

*Figure 28: TEM micrographs of doped hybrid glass 65%MTES-35%DMDES surface (up), 70%MTES-30%DMDES (down) cross section*

the nanoparticles. Dielectric constant, thickness of the coating and agglomerated nanoparticles are some the variables that cause these changes. The intensity shown in the spectra is not directly correlated with the concentration of the nanoparticles, because the thickness of the coating varied.

Evidence of the presence of the nanoparticles from the plasmon peak in UV-Vis spectra was confirmed by TEM micrographs. TEM was used to image the doped hybrid glasses. Imaging of melting gels was a demanding task because of the nature of the material. In order to image samples with TEM, microtomed slices of consolidated melting gels were deposited on TEM grids. The images in Figure 28 show that the nanoparticles are monodispersed in the hybrid silica network. Nanospheres are found throughout the surface of the sample and in the cross section. The size of the nanoparticles is also maintained as shown in Figure 28 after their incorporation in the host medium.

Particularly, it is worth noting that the USAXS instrument is primary-calibrated, i.e., the measured intensity is directly related to the differential scattering cross section, a physical property of the material being studied. All precursor ratio melting gels showed very good mixing and structure correlation is weak and confined to nm scale. The correlation length, identified by Debye-Bueche model, is approximately 6.1 nm. No large-scale structure inhomogeneity exists in non-doped melting gels. For doped melting gels the size of Au-nsps follows a Gaussian distribution with a nominal radius of 15.8 nm and Gaussian width of 5.5 nm. Aggregates were detected with SAXS that have a nominal size (radius) of 190.6 nm.

Raman spectroscopy is the last of the characterization techniques used to study the composite material. As a complementary method of analysis to FT-IR, Raman was used to investigate the structure of consolidated melting gels.

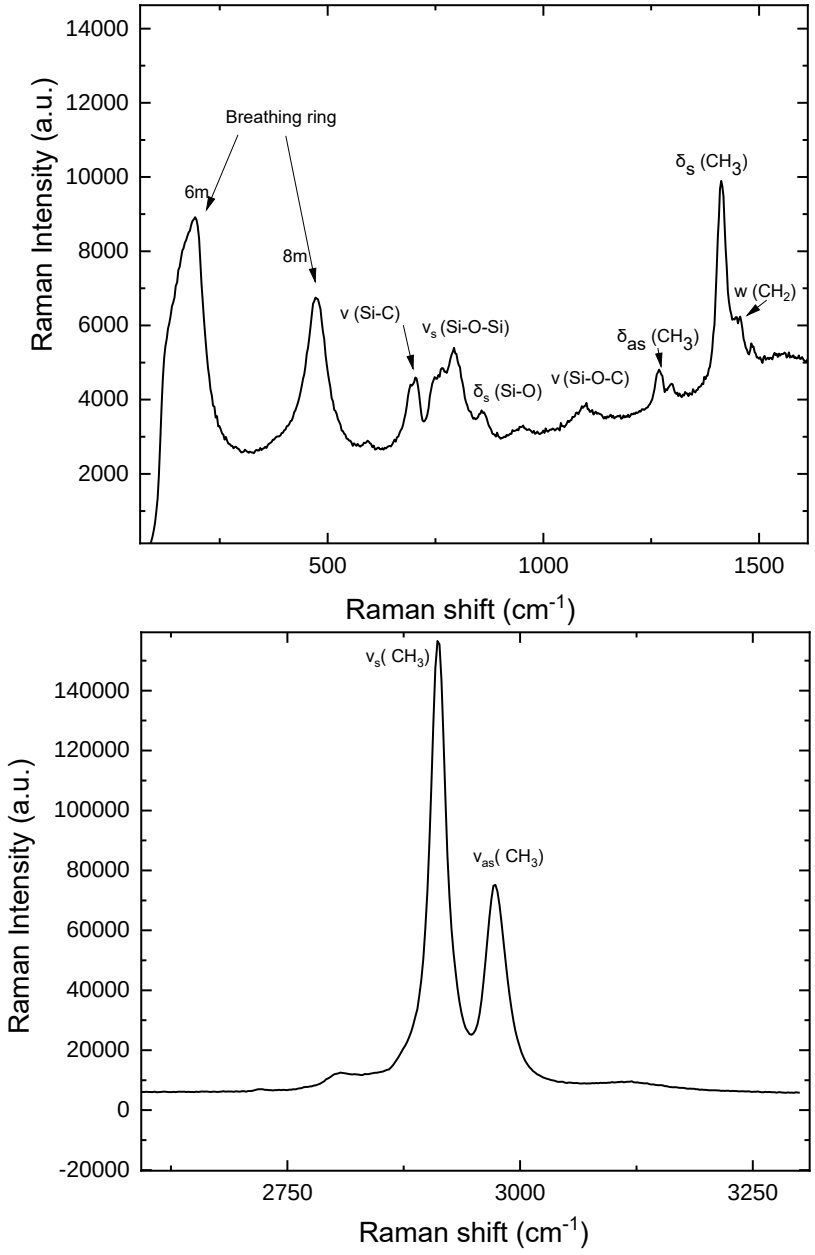


*Figure 29: Raman spectra of 65%MTES-35%DMDES consolidated melting gel collected with 532nm laser at 10% power*

The spectra revealed the presence of 6-member and 8-member breathing rings which is expected to appear in this type of material. The $v_S(CH_3)$ and $v_{as}(CH_3)$ were the two peaks with the highest intensity in the spectra as shown in Figure 29. In the figure above the two areas of interest present the assigned vibrational modes.

Figure 30 shows the spectra collected from hybrid silica glasses with and without nanoparticles. One of the differences between doped and undoped spectra was the fluorescence in the case of undoped melting gel, which created difficulties in the measurements.

*Table 8: Peak assignments for Raman spectra of 65%MTES-35%DMDES consolidated melting gel collected with 532nm laser at 10% power*

| **Peak Assignment** | **Raman Shift ($cm^{-1}$)** |
|---|---|
| Breathing Ring 6m | 189 |
| Breathing Ring 8m | 471 |
| v(Si-C) | 705 |
| $V_s$(Si-O-Si) | 797 |
| $\delta_s$(Si-O) | 861 |
| v(Si-O-C) | 1096 |
| $\delta_{as}(CH_3)$ | 1271 |
| $\delta_s(CH_3)$ | 1413 |
| w($CH_2$) | 1454 |
| $v_s(CH_3)$ | 2911 |
| $v_{as}(CH_3)$ | 2972 |

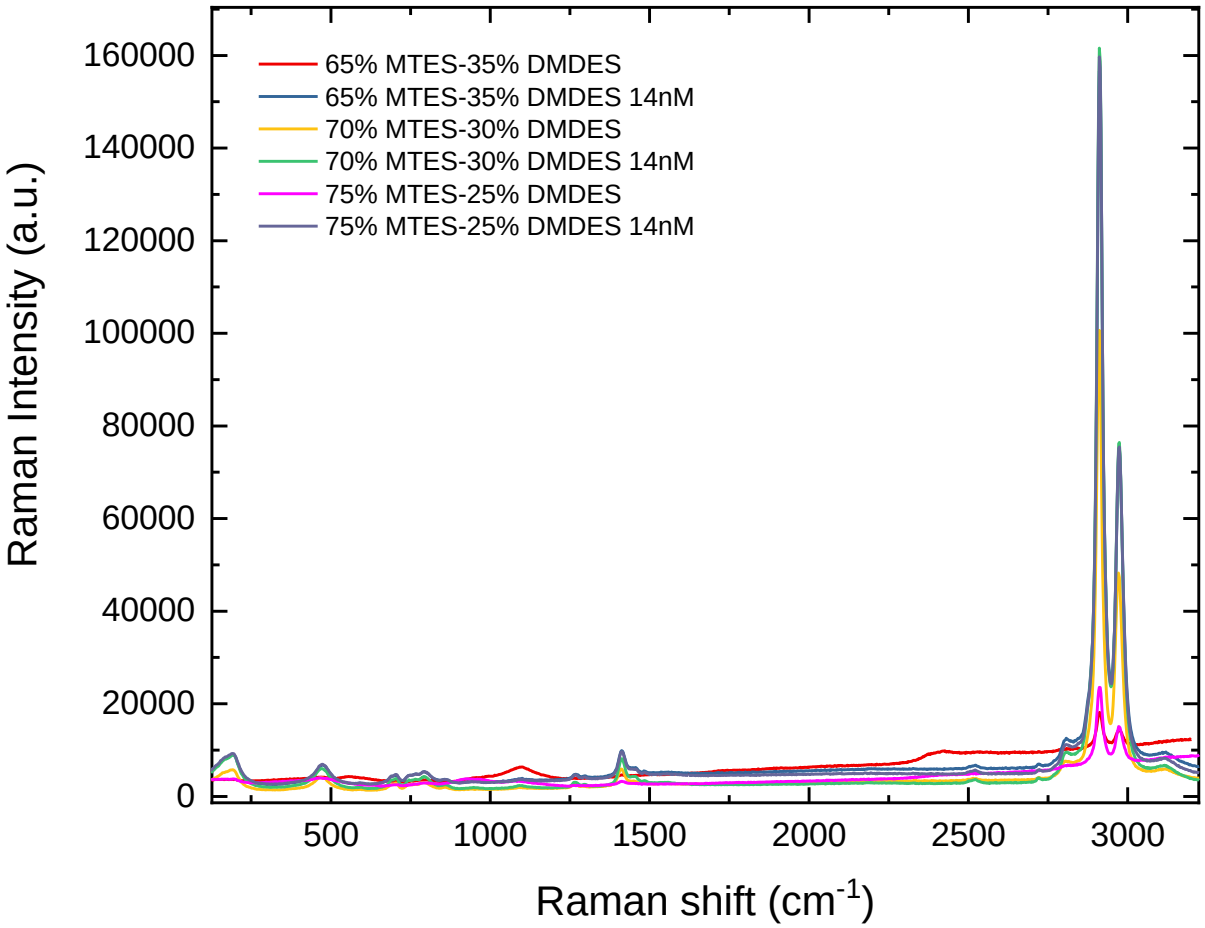


*Figure 310: Raman spectra of 65%MTES-35%DMDES, 70%MTES-30%DMDES,75%MTES-25%DMDES hybrid silica glasses non-doped and doped with 14 nM Au-nsps collected with 532nm laser at 10% power.*

# Discussion

The results of this study show that the new composite material, where gold nanospheres are embedded in a melting gel matrix, maintains the key characteristics of its two components. The gold nanospheres maintain their plasmonic resonance, and the melting gels maintain their softening behavior. The main characteristics of melting gels and gold nanospheres were combined with little effect on either one.

One of the goals of this project was to uniformly dope melting gels with monodisperse gold nanoparticles. Initially, the study of gold citrate nanospheres proved that this type of nanoparticles is stable in acetone. Their stability was determined with UV-Vis spectroscopy, which showed no alterations in the shape and position of the plasmon peak of the nanoparticles. The plasmon peak corresponds to a characteristic shape and size of nanoparticles. Finally, based on the analysis with DLS and the appearance in TEM, it is confirmed that the dispersion of nanoparticles used to dope melting gels had a narrow size distribution of the monodispersed nanospheres.

Melting gels with three ratios of precursors were studied in detail. The first analysis of their structure involved measuring their viscosity as a function of composition and temperature. The method used was oscillatory rheometry, which was used to measure the viscous and elastic moduli, and the glass transition temperature.

In the case of viscosity, the results were different for each ratio of precursors. The samples with the highest organic content (65%MTES-35%DMDES) showed a decrease in the viscosity for all of the doped samples compared to the undoped melting gel. For this composition, as shown below in Figure 31, the viscosity and $T_g$ follow a similar trend. In comparison, 70%MTES-30%DMDES shows a steady increase in the viscosity with an

exception of the 12nM gold nanospheres concentration that decreases slightly compared to the other five nanoparticle concentrations. The melting gel with the lowest organic content (75%MTES-25%DMDES) had the opposite trend to 65%MTES-35%DMDES, where its viscosity went through a maximum at 10nM gold nanospheres and then decreased with the lowest value observed at the highest nanoparticle concentration.

Table 9 and Figure 32 below show the $T_g$ values of all three compositions obtained by Oscillatory Rheometry and Differential Scanning Calorimetry. The graph shows that the values are not identical but they do follow the same trend for each gold nanospheres concertation. The 75%MTES-25%DMDES composition appears to have the closest match in values between the two methods. Oscillatory rheometry was performed multiple times on selected samples. The samples selected covered all three precursor ratios and varied in concentration of gold nanoparticles. The oscillatory rheometry measurements were

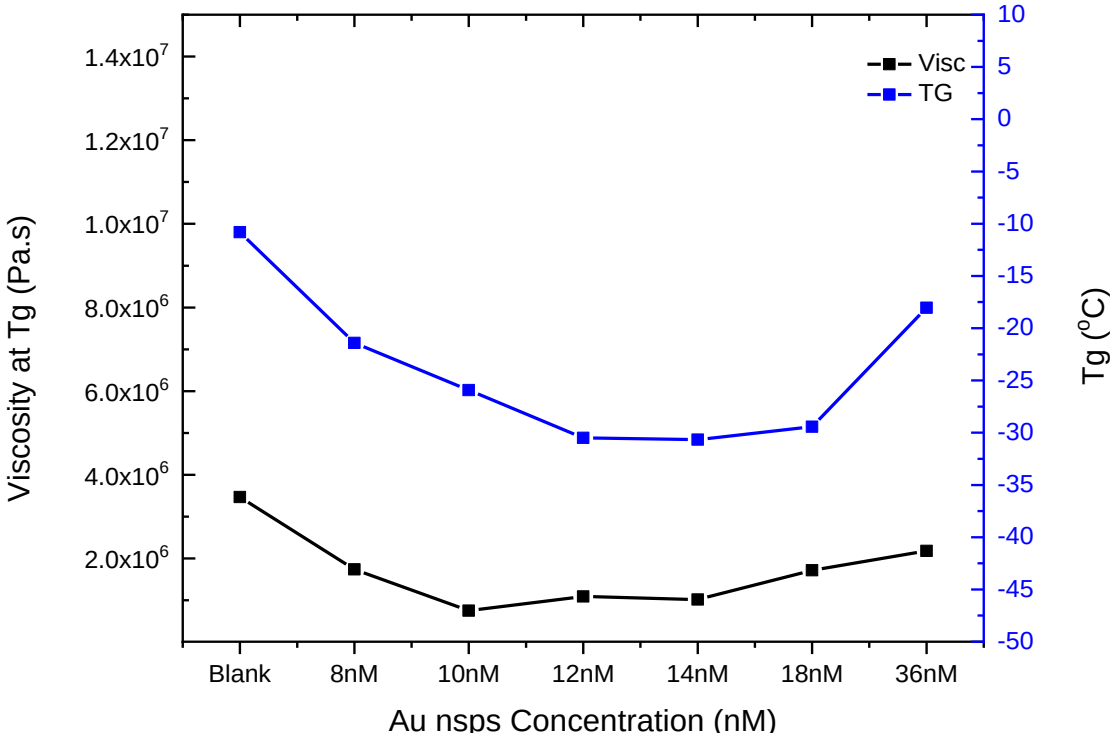


*Figure 32: 65%MTES- 35%DMDES melting gel Viscosity and $T_g$ with respect to the Au-nsps concentration collected with oscillatory rheometry.*

repeated on some samples multiple times. For selected compositions the measurements were repeated on samples synthesized in different batches. The results reported in this study are the repeatable results of these measurements as the values of viscosity and $T_g$ were the same for every measurement of the selected compositions.

*Table 9: $T_g$ of 65%MTES-35%DMDES, 70%MTES-30%DMDES, 75%MTES-25%DMDES obtained by Oscillatory Rheometry (OR) and Differential Scanning Calorimetry (DSC)*

| Au-nsps C (nM) | 65%MTES-35%DMDES $T_g$ (°C) OR | 65%MTES-35%DMDES $T_g$ (°C) DSC | 70%MTES-30%DMDES $T_g$ (°C) OR | 70%MTES-30%DMDES $T_g$ (°C) DSC | 75%MTES-25%DMDES $T_g$(°C) OR | 75%MTES-25%DMDES $T_g$ (°C) DSC |
|---|---|---|---|---|---|---|
| **0 nM** | -10.82 | -26.01 | -8 | -10.24 | 2.1 | 4.55 |
| **8 nM** | -21.4 | -28.19 | -5.4 | -7.06 | -1.49 | -3.73 |
| **10 nM** | -25.92 | -30.53 | -13.6 | -20.02 | -2.96 | -6.44 |
| **12 nM** | -30.5 | -31.7 | -7.6 | -9.06 | -6.5 | -9.95 |
| **14 nM** | -30.66 | -29.41 | -14.64 | -24.4 | -3.83 | -8.06 |
| **18 nM** | -29.42 | -29.82 | -13.5 | -20.78 | -3.02 | -7.4 |

In order to ensure that the glass transition temperature values are reproducible by DSC the measurements were repeated following the same route as for the oscillatory rheometry measurements. DSC measurements were performed multiple times to samples of the same and different batches of the selected compositions. The reported values are the final and reproducible values of $T_g$ obtained by DSC.

The use of two analytical techniques allowed the confirmation of the melting gel behavior while increasing the concentration of the nanoparticles. Another observation

is that the highest and lowest organic content melting gels follow the same trend, which is a decrease in $T_g$ with an increase of gold nanospheres. Regarding these data, it is

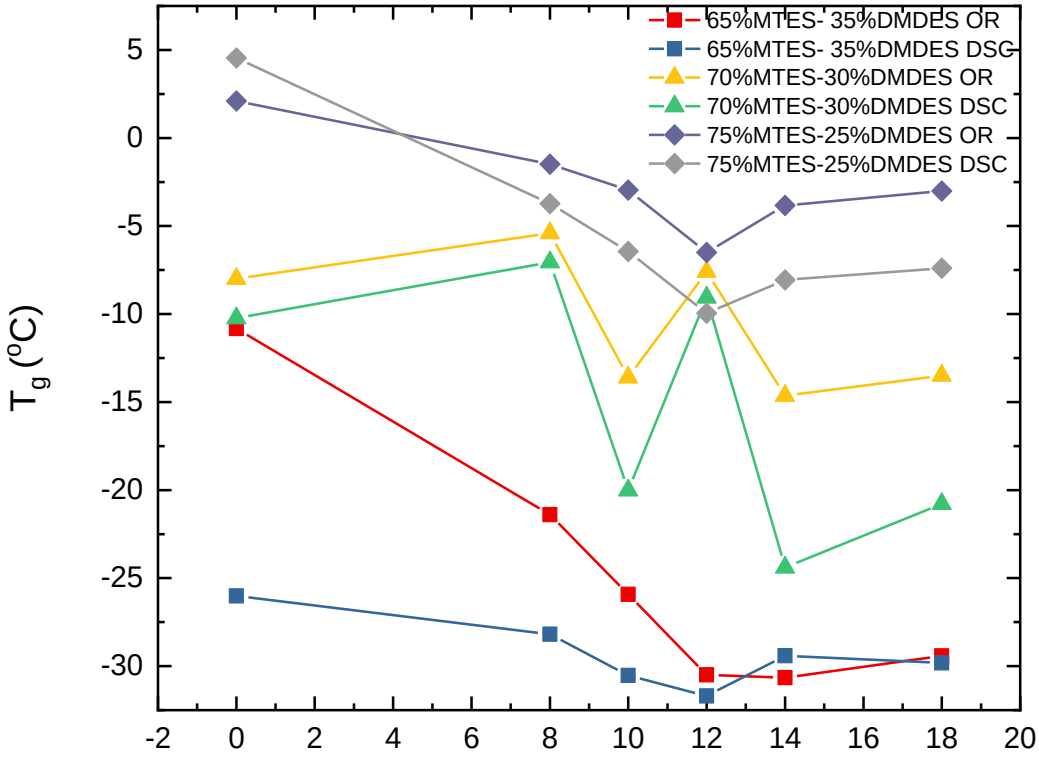


*Figure 35: $T_g$ of 65%MTES-35%DMDES, 70%MTES-30%DMDES,75%MTES-25%DMDES obtained by Oscillatory Rheometry (OR) and Differential Scanning Calorimetry (DSC)*

evident that gold nanoparticles lower the $T_g$ for those two melting gel compositions. The glass transition temperature is associated with chain stiffness for polymer materials. As melting gels are hybrid silica gels consisting of siloxane chains that are formed during the sol-gel process, $T_g$ represents the stiffness of the siloxane chains. Higher content of methyl groups means fewer hydrolyzable groups capable of forming links between siloxane chains. The higher the percentage of ethoxy groups is, the more that polysiloxanes are formed. The Si-$CH_3$ bonds in the network prevent crosslinking of the polysiloxane chains into three-dimensional network.

A low glass transition temperature is indicative of the hybrid silica network having more linear polymeric chains. Taking that into consideration, it is reasonable to suggest that gold nanospheres interfere with the formation of the silica network. For the samples that had lower $T_g$ than the undoped melting gels, it follows that the nanoparticles inhibited the crosslinking of the chains resulting in more linear networks. This trend for glass transition temperature agrees with the viscosity results, since a more linear network has lower viscosity.

Further results from the thermal analysis of the samples with TG-DTA showed that the samples with nanoparticles had decreased total mass loss percentage than samples without nanoparticles. A logical explanation is that the doped melting gels contain nanoparticles that do not decompose in the temperature range that the analysis is performed. The difference between doped and undoped samples was larger as the organic content of the network increased. Since the analysis was performed on the same nanoparticle concentration, the difference is associated with the precursor ratio. From Table 6 it is seen that the mass loss percentage is higher for higher percentage of di-substituted precursor. As described in the results, the thermal decomposition of melting gels involves removal of the residual ethoxy groups and combustion of methyl groups. Both groups are in higher concentration in the 65%MTES- 35%DMDES which leads to higher mass loss.

The DTA curves showed a shift of the second exotherm to higher temperatures for the samples that contained gold nanoparticles. That exotherm peak is associated with the combustion of methyl groups, which are the main source of organic matter. The capping agent of the gold nanospheres is citrate, which is a more complex molecule containing methyl groups. A shift to higher temperatures could be attributed to the

citrate content of the doped melting gels which requires higher temperatures for its thermal decomposition. However, the concentration of nanospheres is small, so it is hard to determine whether or not the citrate capping has an effect on the exothermal peak.

A closer look into the structural analysis of melting gels was performed with the help of FT-IR and Raman spectroscopies. In order to see how the network changed during the consolidation process, the area of the spectra that has the most data was

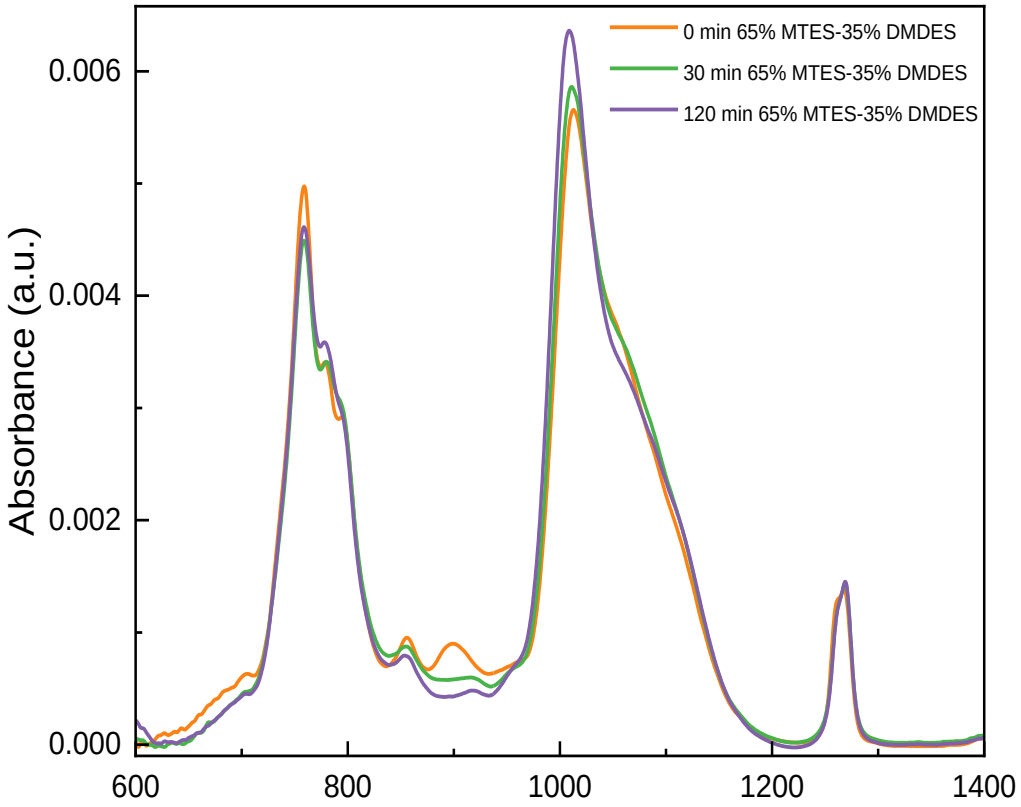


*Figure 33: spectra of 65%MTES- 35%DMDES melting gel at 0min- 25°C, 30min- 150°C and 120min- 150°C after 90 minutes.*

analyzed in detail. In Figure 33, the area of 600-1400 $cm^{-1}$ is presented for the spectra at room temperature, upon reaching the consolidation temperature, the beginning of the consolidation process and after ninety minutes of isothermal treatment at the

consolidation temperature. Immediately, it is evident that there are differences in the in the intensity and position of the peaks.

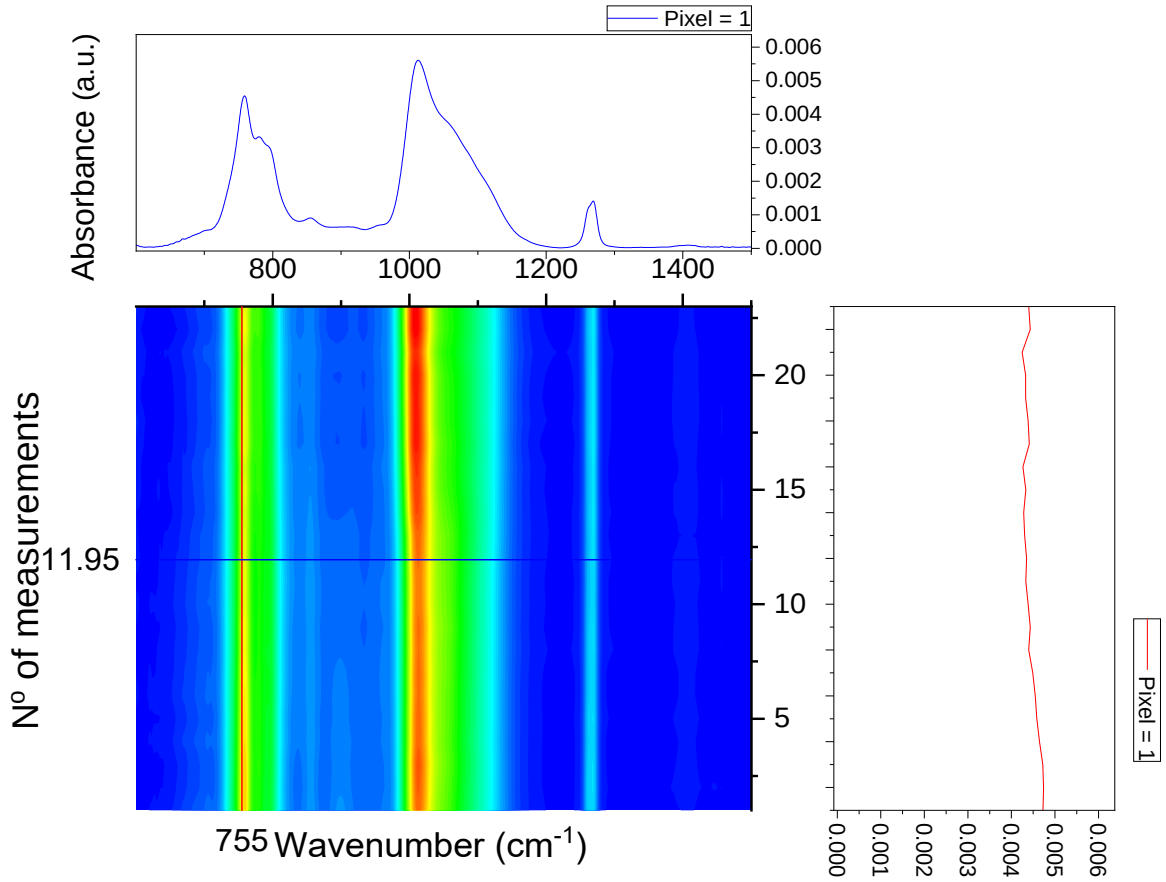


*Figure 34: contour map of spectra intensity with time of 65%MTES- 35%DMDES melting gel from the FT-IR spectra during the monitoring of the consolidation process from 25°C to 150°C.*

In an effort to study the evolution of this process the intensity of selected peaks was mapped with respect to the spectra at room temperature. Figure 33 shows how the intensity of the spectra changes with time for the area 600-1400 $cm^{-1}$. The peaks that were chosen for analysis are characteristic of the amorphous silica network. First is the peak assigned to symmetric vibrational mode of Si-O-Si at 758 $cm^{-1}$. Second is the asymmetric vibrational mode of Si-O-Si transverse (TO) at 1012 $cm^{-1}$, and third is the asymmetric vibrational mode of Si-O-Si longitudinal (LO). These three peaks were

monitored through two stages of the consolidation process, during the heating ramp which was the first thirty minutes, and isothermal heating at the consolidation temperature. Figure 34 shows the changes in intensity for the three peaks with respect to time. From minute 23 to 120, the samples are at a constant temperature at 150°C. In Figure 35, it is seen that the there is a change in the intensity when the samples reach a certain temperature. Samples with gold nanospheres showed a change in the intensity trend for the symmetric vibrational mode earlier than undoped samples. For 65%MTES-35%DMDES, the non-doped melting gels reaches a minimum at 30 minutes at 150°C (7 mins at $T_{con}$), whereas doped 65%MTES- 35%DMDES reaches a minimum at 23 minutes at 150°C (0 mins at $T_{con}$). The 70%MTES-30%DMDES melting gel had a minimum at 140°C (at 0 mins at $T_{con}$) while doped 70%MTES-30%DMDES had a minimum at 21 min at 130°C. For 75%MTES-25%DMDES, the minimum is at 19 minutes at 120°C and the doped sample at 15 minutes at 100°C. Similar delay is observed for the minimum of $\nu_{as}$ Si-O-Si TO, where 65%MTES-35%DMDES and 75%MTES-25%DMDES have a minimum at 19 minutes and 120°C, and the doped melting gels have a minimum at 100°C. The small delay observed in the intensity change is related to the characteristics of the 3D network.

After the absorbance spectra were obtained by FTIR a baseline correction was applied according to the temperature that the sample was when the spectrum was collected. In order to study the evolution of the consolidation process the spectra were the plotted in contour plots as shown in Figure 34. The contour plots show how the intensity of the spectrum changes with respect to time. The x axis corresponds to wavelength and the y axis shoes the consecutive number of the spectrum, this corresponds to a specific time during the consolidation process. After the selection of the peaks that expressed the changes of the hybrid network the intensity of each spectrum throughout the heating

ramp was obtained. The intensity of the each measurement was divided by the intensity of the initial measurement in order to study the trend of the absorbance intensities as shown I Figure 35.

The consolidation process is evolving by the formation of a more complex three-dimensional network. During this process, uncondensed parts of the network come to a favorable position that allows further condensation reactions. Studies have shown that 4-fold and 6-fold rings are formed in a silica network.[43] Also from Raman spectroscopy, there is evidence for the presence of 8-fold rings in the consolidated melting gels. The higher degree of crosslinking means that the range of angles of Si-O-Si is wider because the stiffness of the material increases. The wider range of angles creates a material that is more amorphous, and the asymmetric vibrational modes are favored, which is the case with $v_s$ Si-O-Si and $v_{as}$ Si-O-Si TO.

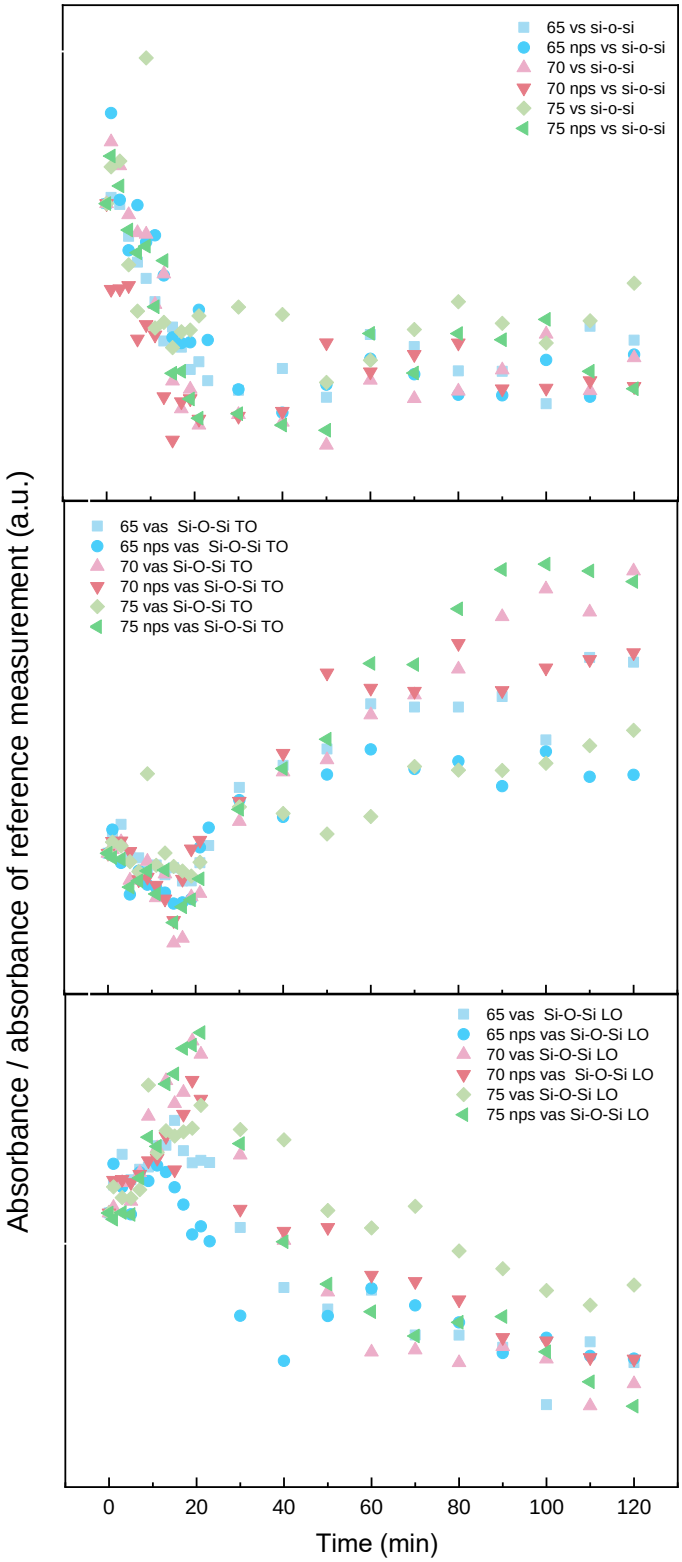


*Figure 35: intensity tracking of vs Si-O-Si, vas Si-O-Si TO and vas Si-O-Si LO of 65%MTES-35%DMDES, 70%MTES-30%DMDES, 75%MTES-25%DMDES melting gels with respect to time*

In contrast, LO modes are not that intense because electromagnetic waves have transverse electric fields and they cannot couple directly. According to Primeau et. al. LO modes propagate through pores, which explains the trend seen in the third graph in Figure 35. What is happening is that as the material crosslinks, the porosity of the glass decreases and the LO band intensity lowers. [89]

Interpretation of FT-IR spectroscopy for silicate materials historically has been problematic for some areas. The most common area that is problematic is 900 to 1200 $cm^{-1}$ because several vibrational modes have been assigned in that region. Taking into consideration an overview of the assigned peaks and the peaks found in these spectra, a deconvolution of the aforementioned region is necessary. Based on the second

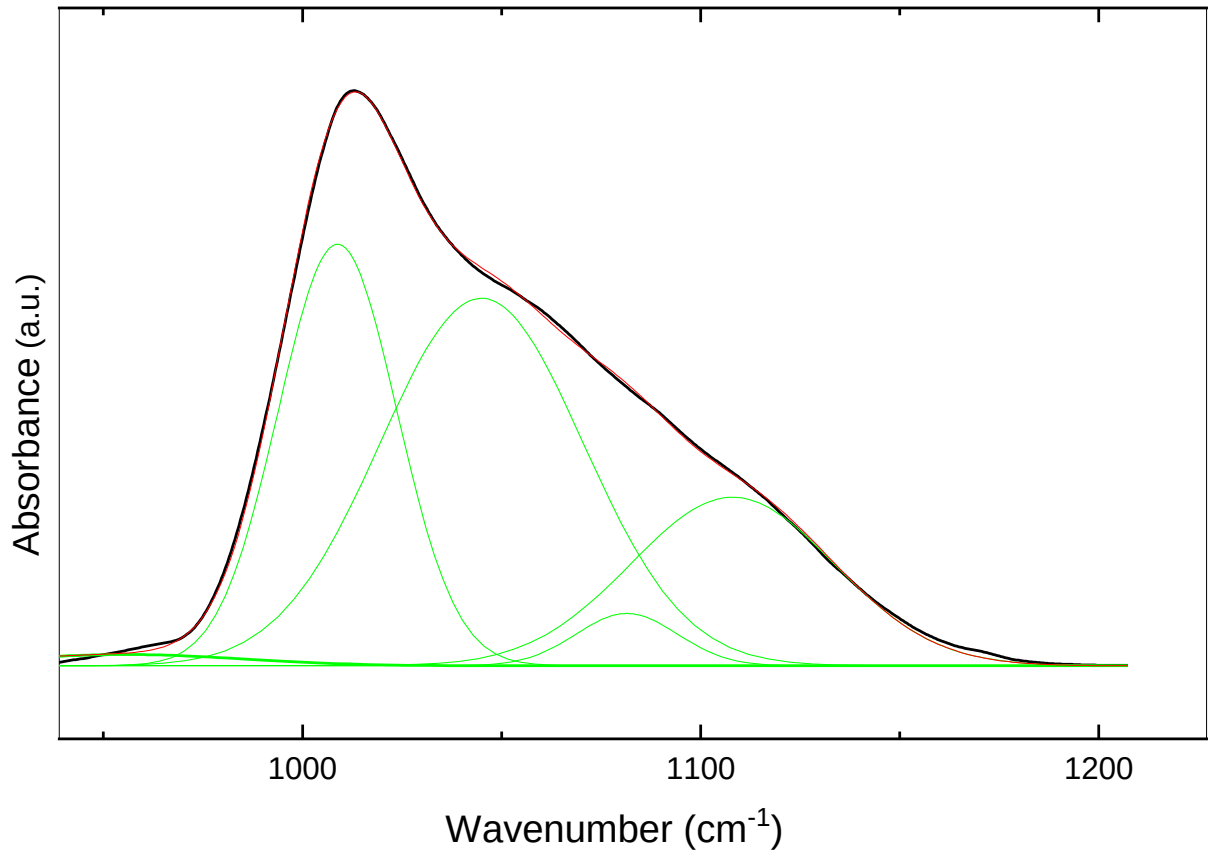


*Figure 3639: Deconvolution of 900-1200 $cm^{-1}$ area of 65%MTES-35%DMDES melting gel to five discreet peaks*

derivative of spectra and the application of Savitzky-Golay method of smoothing the result was five peaks as shown in Figure 36 and Table 10.

*Table 10: Data of peak deconvolution for 900-1200 cm-1 area of 65%MTES-35%DMDES melting gel*

| Peak Index | Peak Type | Area | FWHM | Peak Position |
|---|---|---|---|---|
| 1 | Gaussian | 0.00333 | 23.9907 | 957.32312 |
| 2 | Gaussian | 0.20044 | 38.85238 | 1011.32157 |
| 3 | Gaussian | 0.02744 | 30.86264 | 1041.44039 |
| 4 | Gaussian | 0.10987 | 49.79723 | 1056.55802 |
| 5 | Gaussian | 0.13312 | 72.47296 | 1098.62295 |

First, it is noticed that the positions of the peaks are different from the ones that are usually assigned. Another issue is the peak position with respect to the temperature, which could be resolved from peak deconvolution of the spectra. The TO and LO modes positions are sensitive to stoichiometry, strain and structural features. Primeau et. al. stated that TO is affected by temperature, as the temperature increases the peak shifts to lower wavenumbers.[89] Further investigation of this area will provide useful data for the nature of the hybrid silica network.

Raman spectroscopy showed that the samples that were doped had better quality spectra without any fluorescence interfering with the spectra. In particular, the biggest problem was with 65%MTES-35%DMDES hybrid glasses, which had the highest fluorescence of the three precursor ratios. Among the spectra, no shift in the peaks were recorded for any of the samples. The absence of change indicates that doped and

undoped melting gels created a hybrid glass that has essentially the same structure as a final product. The hybrid glass containing gold nanospheres shows differences in the structure while it is still in the gel form, but these differences disappear, according to Raman spectroscopy.

Melting gels with the addition of nanoparticles have acquired the property of optical limiting in the UV-Vis range of the electromagnetic spectrum. Using TEM and UV-Vis spectroscopy the morphology of the nanoparticles and their plasmonic properties were studied. UV-Vis spectra were collected for comparison between the concentrations of gold nanospheres and precursor ratios. The results showed the appearance of a plasmon peak at the spectra of doped hybrid glasses. The peak was shifted from its position at 520nm, which is for gold nanospheres dispersed in water, to 568nm.

The dielectric properties of the host material and the thickness of the coating were the critical parameters for the intensity of the peaks. Because the coatings are made by hand, they do not have uniform thickness, which means different path lengths, making direct comparisons of intensities impractical.

The absorbance of UV-Vis spectrums of the hybrid glasses presents some negative values for some the samples. This happens due to problems or misalignment of the spectrophotometer components. This negative absorbance is evident in various different compositions of samples without any preference to a specific precursor ratio of the hybrid glass. The fact that this negative absorbance was observed in multiple days and samples needs to be considered. The focus should be on the curve from plasmon appearance that is visible for all the doped samples and not the intensity of the absorbance.

The nanoparticles were imaged successfully in all three precursor composition with no noticeable differences among the samples, in terms of particle size or distribution. All of the samples contained monodisperse gold nanospheres throughout the bulk of the material. Among the samples that were analyzed, there was no evidence of changes of shape and size of the nanoparticles. That confirmed the major result that gold nanoparticles were incorporated in a hybrid organic-inorganic silicate. Unlike other reports of the incorporation of gold nanospheres in ORMOSILs, this was accomplished without any alteration of the gold nanosphere surfaces or a pretreatment with silica or polymer coating. SAXS though reported the appearance of both monodispersed Au-nsps and nanoparticle aggregations. The size of the nanoparticles after the incorporation and consolidation process was reported unchanged.

# Conclusion

This study showed that melting gels and gold nanospheres can be combined in a nanocomposite material. Hybrid organic-inorganic silica networks from different precursor ratios were successfully used as a host material for the nanoparticles. The method of incorporation used only solvent exchange to facilitate a smooth transition from water-dispersed particles to gel-dispersed particles. An uncommon method because of the instability of the nanoparticles which usually are coated with silica before their addition to any silicate network or glass like material.

A new material that has maintained the most noteworthy characteristics of its components was created. The doped melting gels after the addition of nanoparticles continue to exhibit the softening- become rigid- re-softening behavior. Gold nanospheres also maintained the plasmon resonance of the surface electrons and delivered it to the composite material. Plasmonic resonance is present to the consolidated hybrid glass. As the nanoparticle concentration increased the intensity of the color of the doped melting gels increases which means that a controlled thickness the absorbance can be tuned by using different concentrations of nanoparticles. The material that was created is used as corrosion protection layer. Now that melting gels with absorbance in the UV-Vis are available the material could be using for protection from light in the UV-Vis range. This first attempt of doping melting gels with nanoparticles can be used as a base to incorporate different types of nanoparticles.

Thermal analyses and oscillatory rheometry showed changes in the viscosity, glass transition temperature and mass loss when the nanoparticles were introduced in the system. Doped melting gels in total had lower mass loss percentage through the process

of heating in air. Coatings for corrosion protection are benefited by low mass loss since they have to be durable and last as much as they can. An investigation of the viscosity trends with regard to the nanoparticle concentration was performed. The results did not show a clear trend that includes all the precursor compositions, but there is a correlation between the amount of di-substituted precursors in the melting gel. As the percentage of DMDES increased the viscosity seemed to be decreasing as the concentration of nanoparticles increased. Depending on the application the correct nanoparticle concentration can be chosen for higher or lower viscosity of a specific precursor ratio. The glass transition temperatures of doped melting gels seemed to have similar trends for 65%MTES-35%DMDES and 75%MTES-25%. These two compositions went through a minimum at 12nM Au-nsps and then the glass transition temperature increased again. Based on the $T_g$ observations both from DSC and oscillatory rheometry the nanoparticles inhibit the crosslinking of the material creating linear chains rather than 3D network.

Structural investigation with FT-IR showed that nanoparticles make the consolidation process to initiate earlier. A faster consolidation process can lower the energy cost needed to create the hybrid silica coating. Another finding is the deconvolution of the 900 -1200 $cm^{-1}$ area that showed the overlapping of five distinct peaks. The analysis of this area can give information for the evolution of the consolidation process. $v_{as}$ Si-O-Si transverse (TO) and longitudinal (LO) depend on structure , stoichiometry and strain that are characteristics of the silica network. Raman spectroscopy also gave us information for the structure of the silica network. Although from $T_g$ values it was found that the nanoparticles create a more linear network no differences were found in the position of the peaks. That leads to conclude that the structural differences are prominent only while the hybrid silica network is still in the gel

form and the final material does not have differences among precursor compositions and nanoparticle concentrations. Nanoparticles solved the fluorescence problem and provided better quality spectra.

In conclusion, the new nanocomposite material has combined successfully the two components creating an enhanced version of corrosion protection coatings. The nanoparticles succeeded in the task of homogeneous dopant and created a coating that can be tuned regarding its absorbance intensity and viscosity. Evidence show also that doped melting gels need less time to transform into hybrid silica glasses.

# Future Work

This study is the first step towards doping melting gels with nanoparticles. The potential of melting gels as a host for nanoparticles was proven by many types of analyses. This area of research, though, could be broadened by further investigations with gold nanoparticles or other types of metals. This project used nanospheres as nanoparticle dopant, one of the next steps would be the incorporation of different types of nanoparticles. Different shapes of gold nanoparticles should be tested for the modification of melting gels. The incorporation of gold nanorods or nanostars should contribute in the exploration of the preferred dopant shape. Also, this investigation would answer whether the silica network causes changes on the nanoparticle shape after doping. A comparison among different types of metal nanoparticles with the same size and surface chemistry would illuminate the effect of different metals on the hybrid silica network.

Further investigation of the particular systems studied in this project would provide more information about the interface of the two components of the system. A 12 hour monitoring of the consolidation process with FT-IR would provide a more comprehensive idea of the changes during the process. Also, a Raman analysis on melting gels during the consolidation process might answer how the gels transition to a hybrid glass by focusing on the 6 and 8 silicone member rings.

As corrosion protection coatings, melting gels should be studied for efficiency of the coating on metal and polymer surfaces. This investigation between doped and non-doped melting gels would show whether the nanoparticles create a better anticorrosive

coating. Preliminary studies on polymers showed that because of the absorption band in the UV-Vis doped melting gels offer protection from UV-light. Additional experiments towards this hypothesis would confirm the protection of metals and photosensitive polymers by doped melting gels.

In conclusion, this study can be used as the base on which research on melting gel doping can expand. In depth structural analysis will offer useful insight on how the silica network is formed and why melting gels have this softening behavior until they permanently transform to glass.

# References


1. Schmidt, H., Organically Modified Silicates By The Sol-Gel Process. *MRS Proceedings.* **1984,** *32*.
2. Katagiri, K.; Hasegawa, K.; Matsuda, A.; Tatsumisago, M.; Minami, T., Preparation of Transparent Thick Films by Electrophoretic Sol-Gel Deposition Using Phenyltriethoxysilane-Derived Particles. **1998**
*81* (9), 2501-2503.
3. Aparicio, M.; Jitianu, A.; Rodriguez, G.; Degnah, A.; Al-Marzoki, K.; Mosa, J.; Klein, L. C., Corrosion Protection of AISI 304 Stainless Steel with Melting Gel Coatings. *Electrochimica Acta* **2016,** *202* (Supplement C), 325-332.
4. Pandey, P., A review on ormosil-based biomaterials and their applications in sensor design. *Journal of the Indian Institute of Science* **2013,** *79* (5), 415.
5. Yang, J.; Chen, J.; Song, J., Studies of the surface wettability and hydrothermal stability of methyl-modified silica films by FT-IR and Raman spectra. **2009,** *50* (2), 178-184.
6. Jitianu, A.; Doyle, J.; Amatucci, G.; Klein, L. C., Methyl-modified melting gels for hermetic barrier coatings. *Proceedings MS&T* **2008**, 2171-2182.
7. Link, S.; El-Sayed, M. A., Size and temperature dependence of the plasmon absorption of colloidal gold nanoparticles. *The Journal of Physical Chemistry B* **1999,** *103* (21), 4212-4217.
8. Alemán, J. V.; Chadwick, A. V.; He, J.; Hess, M.; Horie, K.; Jones, R. G.; Kratochvíl, P.; Meisel, I.; Mita, I.; Moad, G.; Penczek, S.; Stepto, R. F. T., Definitions of terms relating to the structure and processing of sols, gels, networks, and inorganic-organic hybrid materials (IUPAC Recommendations 2007). In *Pure and Applied Chemistry*, 2007; Vol. 79, p 1801.
9. Ebelmen, Untersuchungen über die Verbindungen der Borsäure und Kieselsäure mit Aether. **1846,** *57* (3), 319-355.
10. Schmidt, H.; Seiferling, B., Chemistry And Applications Of Inorganic-Organic Polymers (Organically Modified Silicates). *MRS Proceedings* **1986,** *73*.
11. Chen, K. C.; Tsuchiya, T.; Mackenzie, J. D., Sol-gel processing of silica. *J Non-Cryst Solids* **1986,** *81* (1-2), 227-237.
12. Zheludkevich, M.; Salvado, I. M.; Ferreira, M., Sol–gel coatings for corrosion protection of metals. *Journal of Materials Chemistry* **2005,** *15* (48), 5099-5111.
13. L. C. Klein, A. D., K. Al-Marzoki, G. Rodriguez, A. Jitianu, Electrochemical Properties of Melting Gel Coatings. *Advances in Materials Science for Environmental and Energy Technologies V* **2016,** *260*, 235.
14. Amberg-Schwab, S.; Katschorek, H.; Weber, U.; Hoffmann, M.; Burger, A., Barrier Properties OF Inorganic-Organic Polymers: Influence of Starting Compounds, Curing Conditions and Storage-Scaling-Up to Industrial Application—. *Journal of Sol-Gel Science and Technology* **2000,** *19* (1), 125-129.
15. Joshua Du, Y.; Damron, M.; Tang, G.; Zheng, H.; Chu, C. J.; Osborne, J. H., Inorganic/organic hybrid coatings for aircraft aluminum alloy substrates. *Progress in Organic Coatings* **2001,** *41* (4), 226-232.
16. Park, M.; Komarneni, S.; Choi, J., Effect of substituted alkyl groups on textural properties of ORMOSILs. *J Mater Sci* **1998,** *33* (15), 3817-3821.

17. Borówka, A., Effects of twin methyl groups insertion on the structure of templated mesoporous silica materials. *Ceramics International* **2019,** *45* (4), 4631-4636.
18. Jitianu, A.; Amatucci, G.; Klein, L. C., Organic–inorganic sol-gel thick films for humidity barriers. **2008,** *23* (08), 2084-2090.
19. Silva, C. R.; Airoldi, C., Acid and Base Catalysts in the Hybrid Silica Sol–Gel Process. **1997,** *195* (2), 381-387.
20. Danks, A. E.; Hall, S. R.; Schnepp, Z., The evolution of 'sol–gel' chemistry as a technique for materials synthesis. *Materials Horizons* **2016,** *3* (2), 91-112.
21. Pope, E. J. A.; Mackenzie, J. D., Sol-gel processing of silica. **1986,** *87* (1-2), 185-198.
22. Vincent, A.; Babu, S.; Brinley, E.; Karakoti, A.; Deshpande, S.; Seal, S., Role of Catalyst on Refractive Index Tunability of Porous Silica Antireflective Coatings by Sol-Gel Technique. **2007,** *111* (23), 8291-8298.
23. Rios, X.; Moriones, P.; Echeverría, J. C.; Luquín, A.; Laguna, M.; Garrido, J. J., Characterisation of hybrid xerogels synthesised in acid media using methyltriethoxysilane (MTEOS) and tetraethoxysilane (TEOS) as precursors. *Adsorption* **2011,** *17* (3), 583-593.
24. Tardy, Y., The chemistry of silica solubility, polymerization, colloid and surface properties, and biochemistry, Ralf K. Iler, 1979. *Sciences Géologiques, bulletins et mémoires* **1982,** *35* (1), 93-93.
25. Schmidt, H., Organically modified silicates by the sol-gel process. *MRS Online Proceedings Library Archive* **1984,** *32*.
26. Dunn, B.; Nishida, F.; Toda, R.; Zink, J.; Allik, T.; Chandra, S.; Hutchinson, J., Advances in dye-doped sol-gel lasers. *MRS Online Proceedings Library Archive* **1993,** *329*.
27. del Monte, F.; Levy, D., Near-infrared dyes encapsulated in sol-gel matrixes. *Chemistry of materials* **1995,** *7* (2), 292-298.
28. Hollins, R. C., Materials for optical limiters. **1999,** *4* (2), 189-196.
29. Spangler, C. W., Recent development in the design of organic materials for optical power limiting. *Journal of Materials Chemistry* **1999,** *9* (9), 2013-2020.
30. Li, D.; Lin, W.; Jiang, N.; Wang, C.; Li, C., Optical limiting property of gold nanorods/ormosil gel glass composites. *Optics Communications* **2019,** *437*, 363-366.
31. Ren, J.; Sun, X.; Wang, Y.; Song, R.; Xie, Z.; Zhou, S.; Chen, P., Controllable Photoluminescent and Nonlinear Optical Properties of Polymerizable Carbon Dots and Their Arbitrary Copolymerized Gel Glasses. *Advanced Optical Materials* **2018**, 1701273.
32. Zheng, C.; Zheng, Y.; Chen, W.; Wei, L., Encapsulation of graphene oxide/metal hybrids in nanostructured sol–gel silica ORMOSIL matrices and its applications in optical limiting. *Optics & Laser Technology* **2015,** *68*, 52-59.
33. Zheng, X.; Feng, M.; Zhan, H., Giant optical limiting effect in Ormosil gel glasses doped with graphene oxide materials. **2013,** *1* (41), 6759.
34. Tripathi, V. S.; Lakshminarayana, G.; Nogami, M., Optical oxygen sensors based on platinum porphyrin dyes encapsulated in ORMOSILS. **2010,** *147* (2), 741-747.
35. Bescher, E.; Mackenzie, J. D., Hybrid organic-inorganic sensors. *Materials Science and Engineering: C* **1998,** *6* (2-3), 145-154.
36. Wu, K.-H.; Wang, J.-C.; Huang, J.-Y.; Huang, C.-Y.; Cheng, Y.-H.; Liu, N.-T., Preparation and antibacterial effects of Ag/AgCl-doped quaternary ammonium-modified silicate hybrid antibacterial material. *Materials Science and Engineering: C* **2019,** *98*, 177-184.
37. Lin, W.; Zheng, J.; Zhuo, J.; Chen, H.; Zhang, X., Characterization of sol-gel ORMOSIL antireflective coatings from phenyltriethoxysilane and tetraethoxysilane:

Microstructure control and application. *Surface and Coatings Technology* **2018,** *345*, 177-182.
38. Pagliaro, M.; Ciriminna, R.; Palmisano, G., Silica-based hybrid coatings. **2009,** *19* (20), 3116.
39. Mascia, L.; Prezzi, L.; Wilcox, G. D.; Lavorgna, M., Molybdate doping of networks in epoxy–silica hybrids: Domain structuring and corrosion inhibition. *Progress in organic coatings* **2006,** *56* (1), 13-22.
40. Yavas, H.; Selçuk, C. D. Ö.; Özhan, A. E. S.; Durucan, C., A parametric study on processing of scratch resistant hybrid sol–gel silica coatings on polycarbonate. **2014,** *556*, 112-119.
41. Iler, R., The chemistry of silica, A Wiley-Interscience publication. John Wiley & Sons: 1979.
42. Rubio, F.; Rubio, J.; Oteo, J. L., A FT-IR Study of the Hydrolysis of Tetraethylorthosilicate (TEOS). **1998,** *31* (1), 199-219.
43. Fidalgo, A.; Ilharco, L. M., The defect structure of sol–gel-derived silica/polytetrahydrofuran hybrid films by FTIR. **2001,** *283* (1-3), 144-154.
44. Gnyba, M.; Keränen, M.; Kozanecki, M.; Kosmowski, B., *Raman investigation of hybrid polymer thin films*. 2005; Vol. 23.
45. de Ferri, L.; Lorenzi, A.; Lottici, P. P., OctTES/TEOS system for hybrid coatings: real-time monitoring of the hydrolysis and condensation by Raman spectroscopy. *Journal of Raman Spectroscopy* **2016,** *47* (6), 699-705.
46. Jitianu, A.; Cadars, S.; Zhang, F.; Rodriguez, G.; Picard, Q.; Aparicio, M.; Mosa, J.; Klein, L. C., 29Si NMR and SAXS investigation of the hybrid organic–inorganic glasses obtained by consolidation of the melting gels. **2017**.
47. Jitianu, A.; Doyle, J.; Amatucci, G.; Klein, L. C., Methyl modified siloxane melting gels for hydrophobic films. *Journal of Sol-Gel Science and Technology* **2010,** *53* (2), 272-279.
48. Murphy, T.; Schmidt, H.; Kronfeldt, H.-D., Use of sol-gel techniques in the development of surface-enhanced Raman scattering (SERS) substrates suitable for in situ detection of chemicals in sea-water. *Applied Physics B* **1999,** *69* (2), 147-150.
49. Fukumi, K.; Chayahara, A.; Kadono, K.; Sakaguchi, T.; Horino, Y.; Miya, M.; Fujii, K.; Hayakawa, J.; Satou, M., Gold nanoparticles ion implanted in glass with enhanced nonlinear optical properties. **1994,** *75* (6), 3075.
50. Bharathi, S.; Nogami, M.; Ikeda, S., Novel electrochemical interfaces with a tunable kinetic barrier by self-assembling organically modified silica gel and gold nanoparticles. *Langmuir* **2001,** *17* (1), 1-4.
51. Akbarian, F.; Dunn, B. S.; Zink, J. I., Surface-Enhanced Raman Spectroscopy Using Photodeposited Gold Particles in Porous Sol-Gel Silicates. **1995,** 99 (12), 3892-3894.
52. Lundén, H.; Liotta, A.; Chateau, D.; Lerouge, F.; Chaput, F.; Parola, S.; Brännlund, C.; Ghadyani, Z.; Kildemo, M.; Lindgren, M., Dispersion and self-orientation of gold nanoparticles in sol–gel hybrid silica–optical transmission properties. *Journal of Materials Chemistry C* **2015,** *3* (5), 1026-1034.
53. Lundén, H.; Lopes, C.; Lindgren, M.; Liotta, A.; Chateau, D.; Lerouge, F.; Chaput, F.; Désert, A.; Parola, S., Efficient reverse saturable absorption of sol-gel hybrid plasmonic glasses. *Optical Materials* **2017,** *69*, 134-140.
54. Pal, S.; De, G., A New Approach for the Synthesis of Au−Ag Alloy Nanoparticle Incorporated SiO 2 Films. **2005,** *17* (24), 6161-6166.

55. Santana, I.; Pepe, A.; Schreiner, W.; Pellice, S.; Ceré, S., Hybrid sol-gel coatings containing clay nanoparticles for corrosion protection of mild steel. **2016**.
56. Tsoulos, T. V.; Fabris, L., Interface and Bulk Standing Waves Drive the Coupling of Plasmonic Nanostar Antennas. *The Journal of Physical Chemistry C* **2018,** *122* (50), 28949-28957.
57. Lundén, H.; Liotta, A.; Chateau, D.; Lerouge, F.; Chaput, F.; Parola, S.; Brännlund, C.; Ghadyani, Z.; Kildemo, M.; Lindgren, M.; Lopes, C., Dispersion and self-orientation of gold nanoparticles in sol–gel hybrid silica – optical transmission properties. **2015,** *3* (5), 1026-1034.
58. Chateau, D.; Liotta, A.; Lundén, H.; Lerouge, F.; Chaput, F.; Krein, D.; Cooper, T.; Lopes, C.; El-Amay, A. A. G.; Lindgren, M.; Parola, S., Long Distance Enhancement of Nonlinear Optical Properties Using Low Concentration of Plasmonic Nanostructures in Dye Doped Monolithic Sol-Gel Materials. **2016,** *26* (33), 6005-6014.
59. Faraday, M., X. The Bakerian Lecture.—Experimental relations of gold (and other metals) to light. *Philosophical Transactions of the Royal Society of London* **1857,** (147), 145-181.
60. Turkevich, J.; Stevenson, P. C.; Hillier, J., Discuss. Faraday Soc. *Discussions of the Faraday Society* **1951,** *11*, *55*.
61. Frens, G., Controlled nucleation for the regulation of the particle size in monodisperse gold suspensions. *Nature physical science* **1973,** *241* (105), 20.
62. Ji, X.; Song, X.; Li, J.; Bai, Y.; Yang, W.; Peng, X., Size Control of Gold Nanocrystals in Citrate Reduction: The Third Role of Citrate. **2007,** *129* (45), 13939-13948.
63. Indrasekara, A. S. D. S., Paladini, B. J., Naczynski, D. J., Starovoytov, V., Moghe, P. V., & Fabris, L., Dimeric Gold Nanoparticle Assemblies as Tags for SERS-Based Cancer Detection. *Advanced healthcare materials,* **2014,** *2* (10), 1370-1376.
64. Pandey, P. C.; Chauhan, D. S., 3-Glycidoxypropyltrimethoxysilane mediated in situ synthesis of noble metal nanoparticles: Application to hydrogen peroxide sensing. *The Analyst* **2012,** *137* (2), 376-385.
65. Reisfeld, R.; Saraidarov, T.; Levchenko, V., Formation and structural characterization of silver nanoparticles in ormosil sol-gel films. *optica Applicata* **2008,** *38* (1).
66. Zhu, Y.; Elim, H. I.; Foo, Y. L.; Yu, T.; Liu, Y.; Ji, W.; Lee, J. Y.; Shen, Z.; Wee, A. T.-S.; Thong, J. T.-L., Multiwalled carbon nanotubes beaded with ZnO nanoparticles for ultrafast nonlinear optical switching. *Advanced Materials* **2006,** *18* (5), 587-592.
67. Franã§Ois, L.; Mostafavi, M.; Belloni, J.; Delaire, J. A., Optical limitation induced by gold clusters: Mechanism and efficiency. *3* (22), 4965-4971.
68. Wang, G.; Sun, W., Optical Limiting of Gold Nanoparticle Aggregates Induced by Electrolytes. **2006,** *110* (42), 20901-20905.
69. Maier, S. A.; Brongersma, M. L.; Atwater, H. A., Electromagnetic energy transport along arrays of closely spaced metal rods as an analogue to plasmonic devices. **2001,** *78* (1), 16.
70. Stockman, M. I., Electromagnetic theory of SERS. In *Surface-Enhanced Raman Scattering*, Springer: 2006; pp 47-65.
71. Saha, K.; Agasti, S. S.; Kim, C.; Li, X.; Rotello, V. M., Gold Nanoparticles in Chemical and Biological Sensing. *Chemical Reviews* **2012,** *112* (5), 2739-2779.

72. Bhamidipati, M.; Cho, H.-Y.; Lee, K.-B.; Fabris, L., SERS-Based Quantification of Biomarker Expression at the Single Cell Level Enabled by Gold Nanostars and Truncated Aptamers. *Bioconjugate Chemistry* **2018**.
73. Matsuda, A.; Sasaki, T.; Hasegawa, K.; Tatsumisago, M.; Minami, T., Thermal softening behavior and application to transparent thick films of poly (benzylsilsesquioxane) particles prepared by the sol–gel process. *J Am Ceram Soc* **2001,** *84* (4), 775-780.
74. Klein, L. C.; McClarren, B.; Jitianu, A., Silica-Containing Hybrid Nanocomposite "Melting Gels". *Materials Science Forum* **2014,** *783-786*, 1432-1437.
75. Klein, L. C.; Jitianu, A., Organic-inorganic hybrid melting gels. *Journal of Sol-Gel Science and Technology* **2010,** *55* (1), 86-93.
76. Becker, H., Polymer microfluidic devices. **2002,** *56* (2), 267-287.
77. Singh, R.; Kumar, R.; Ahuja, I. S., Thermal analysis for joining of dissimilar polymeric materials through friction stir welding. **2017**.
78. Jitianu, A.; Lammers, K.; Arbuckle-Kiel, G. A.; Klein, L. C., Thermal analysis of organically modified siloxane melting gels. *Journal of Thermal Analysis and Calorimetry* **2012,** *107* (3), 1039-1045.
79. Takahashi, K.; Tadanaga, K.; Matsuda, A.; Hayashi, A.; Tatsumisago, M., Thermoplastic and thermosetting properties of polyphenylsilsesquioxane particles prepared by two-step acid-base catalyzed sol-gel process. **2007,** *41* (3), 217-222.
80. Jitianu, A.; Amatucci, G.; Klein, L. C., Phenyl-Substituted Siloxane Hybrid Gels that Soften Below 140 degrees C. *J Am Ceram Soc* **2009,** *92* (1), 36-40.
81. Hays, G. F., Now is the Time. *World Corrosion Organization* **2010**.
82. Van Ooij, W.; Zhu, D.; Prasad, G.; Jayaseelan, S.; Fu, Y.; Teredesai, N., Silane based chromate replacements for corrosion control, paint adhesion, and rubber bonding. *Surface Engineering* **2000,** *16* (5), 386-396.
83. Osborne, J. H.; Blohowiak, K. Y.; Taylor, S. R.; Hunter, C.; Bierwagon, G.; Carlson, B.; Bernard, D.; Donley, M. S., Testing and evaluation of nonchromated coating systems for aerospace applications. *Progress in Organic Coatings* **2001,** *41* (4), 217-225.
84. Zandi-Zand, R.; Ershad-Langroudi, A.; Rahimi, A., Silica based organic–inorganic hybrid nanocomposite coatings for corrosion protection. **2005,** *53* (4), 286-291.
85. Klein, L. C.; Kallontzi, S.; Fabris, L.; Jitianu, A.; Ryan, C.; Aparicio, M.; Lei, L.; Singer, J. P., Applications of melting gels. *Journal of Sol-Gel Science and Technology* **2019,** *89* (1), 66-77.
86. Metroke, T. L.; Kachurina, O.; Knobbe, E. T., Spectroscopic and corrosion resistance characterization of GLYMO–TEOS Ormosil coatings for aluminum alloy corrosion inhibition. **2002,** *44* (4), 295-305.
87. Tiringer, U.; Milošev, I.; Durán, A.; Castro, Y., Hybrid sol–gel coatings based on GPTMS/TEOS containing colloidal SiO2 and cerium nitrate for increasing corrosion protection of aluminium alloy 7075-T6. *Journal of Sol-Gel Science and Technology* **2018,** *85* (3), 546-557.
88. Jitianu, M.; Jitianu, A.; Stamper, M.; Aboagye, D.; Klein, L. C., Melting gel films for low temperature seals. *MRS Online Proceedings Library Archive* **2013,** *1547*, 81-86.
89. Primeau, N.; Vautey, C.; Langlet, M., The effect of thermal annealing on aerosol-gel deposited SiO2 films: a FTIR deconvolution study. *Thin Solid Films* **1997,** *310* (1-2), 47-56.